Llew 830-4-15
NAS1.60:1647
COMPLETED
ORIGINAL

NASA Technical Paper 1647

Description of an Experimental (Hydrogen Peroxide) Rocket System and Its Use in Measuring Aileron and Rudder Effectiveness of a Light Airplane

Thomas C. O'Bryan, Maxwell W. Goode,
Frederick D. Gregory, and Marna H. Mayo

MAY 1980

NASA

42

NASA Technical Paper 1647

Description of an Experimental (Hydrogen Peroxide) Rocket System and Its Use in Measuring Aileron and Rudder Effectiveness of a Light Airplane

Thomas C. O'Bryan, Maxwell W. Goode,
Frederick D. Gregory, and Marna H. Mayo
Langley Research Center
Hampton, Virginia

National Aeronautics
and Space Administration

**Scientific and Technical
Information Office**

1980

SUMMARY

A hydrogen-peroxide-fueled rocket system was intalled on a light, four-place general aviation airplane to provide known moments about the roll and yaw body axes for use in measuring aerodynamic control power for all flight conditions.

The system produced thrust up to about 490 N (110 lbf) (producing either a yawing or rolling moment of 2500 N-m (1840 ft-lbf)) with pilot-controlled firing time totaling about 60 sec per fuel load. A total of 15 flight operations with approximately 20 min of accumulated rocket firing time was accomplished with no major system malfunction. This experience demonstrated the operational readiness of the system for use in spin tests.

Rudder and aileron effectiveness $\left(C_{n_{\delta_r}}\right.$ and $\left.C_{\ell_{\delta_a}}\right)$ were measured by using the rocket-produced moments to balance the aerodynamic control moments for airspeeds somewhat above the stall to near cruise speed (approximately 65 to 100 knots). These results agreed very well with results obtained from dynamic flight maneuvers using the maximum likelihood method of stability derivative extraction. Comparison of the measured derivatives with those obtained by readily available estimation techniques indicated that the estimates for both derivatives differed appreciably from those measured.

INTRODUCTION

This paper presents the results of tests in which measurements of the aileron and rudder control effectiveness of a light plane were made by using a hydrogen peroxide rocket system installed in the airplane. The liquid propellant rocket system, which is controlled directly in an on-off manner by the pilot, was developed both as a research tool and as a spin recovery device. The system is being used in a recently initiated program undertaken by the Langley Research Center of the National Aeronautics and Space Administration (NASA), to study solutions to stall and spin problems of general aviation aircraft. In addition to specific test results, this report covers a discussion of the rocket system itself and the special technique developed to use it for the measurement of the airplane control characteristics.

One of the essential elements for understanding stall and spin problems is an accurate knowledge of the effectiveness of the aerodynamic controls prior to and during the stalled and spinning maneuvers. Although some data are available through static and dynamic wind-tunnel tests of small-scale models, there are essentially no data for the full-scale conditions in free flight. Some limited data on control effectiveness of full-scale aircraft in normal unstalled flight have been obtained by utilizing testing techniques in which the airplanes have had disturbing moments applied to them by rapid movements of the controls or by the deployment of wing-tip parachutes and drop-

pable weights. (See ref. 1.) However, the effectiveness of these techniques has been limited either by the large number of unknown factors involved or by the cumbersome nature of the one-measurement-per-flight type of operation. The subject rocket system was developed as a means of providing multiple moments of a precisely known magnitude and easily controlled duration. This capability was considered to be essential to the practical and effective utilization of flight techniques for measuring the aerodynamic control characteristics of an airplane throughout the various phases of flight involved in the stall and spin maneuvers.

An added feature of this system is that it has the potential for use as a spin recovery system in place of the customary parachute system. Several applications of solid-propellant type rockets as spin recovery devices have been employed in past years for both model and full-scale airplane tests (refs. 2 and 3) in attempts to overcome some of the uncertainties involved in the utilization of a parachute system. Although these rocket systems have been shown to be very effective, they have been hampered by their "single-shot" characteristic, the inability to control duration of the rocket firing during the flight, and the problem of adjusting the thrust level to match a given size airplane or type of spin maneuver. By utilizing a liquid-propellant system, these undesirable aspects of the solid-propellant system are overcome so that an apparently reasonable degree of controlled operational flexibility can be achieved.

Although no specific tests of the rocket system for spin recovery were performed during this program, use of the rocket system did serve to demonstrate its operational readiness for spin recovery tests.

SYMBOLS

In order to facilitate usage of data presented, dimensional quantities are presented both in the International System of Units (SI) and in the U.S. Customary Units within the text and tables and in SI units only in the figures. Masses are presented in kilograms and pounds mass (1 slug = 32.2 lbm). Measurements were made in the U.S. Customary Units, and equivalent dimensions were determined by using the conversion factors given in reference 4.

b wing span, m (ft)

C_l rolling-moment coefficient, $\frac{M_X}{qSb}$

C_n yawing-moment coefficient, $\frac{M_Z}{qSb}$

M_X rolling moment, N-m (lbf-ft)

$M_{X,R}$ rolling moment due to rocket firing, N-m (lbf-ft) ($T \times y$)

M_Z	yawing moment, N-m (lbf-ft)
$M_{Z,R}$	yawing moment due to rocket firing, N-m (lbf-ft) ($T \times y$)
p	static pressure measured by orifices in airplane's airspeed/altitude system, Pa (lbf/ft^2)
Δp	static-pressure error ($p - p_\infty$), Pa (lbf/ft^2)
p_C	rocket chamber absolute pressure, Pa (lbf/ft^2)
p_∞	free-stream static pressure, Pa (lbf/ft^2)
$\frac{\Delta p}{q_C}$	static-pressure error coefficient
q	dynamic pressure, Pa (lbf/ft^2)
q_C	impact pressure, Pa (lbf/ft^2)
S	wing area, m^2 (ft^2)
T	rocket thrust, N (lbf)
V	true airspeed, knots
V_C	calibrated airspeed, knots
V_i	indicated airspeed, knots
y	lateral distance from center line of airplane to center line of rocket nozzles, 5.08 m (16.67 ft)
α	angle of attack, deg or rad
β	angle of sideslip, deg or rad
δ_a	aileron deflection, deg or rad, $\frac{\delta_{a,r} + \delta_{a,\ell}}{2}$
δ_r	rudder deflection, trailing edge left positive, deg or rad
$\delta_{a,\ell}$	left aileron deflection, trailing edge up positive, deg or rad
$\delta_{a,r}$	right aileron deflection, trailing edge down positive, deg or rad
$\Delta\delta_r$	change in rudder deflection, deg or rad
ρ	air density, kg/m^3 ($slugs/ft^3$)

Subscripts:

0	trimmed flight condition
1	test flight condition
j	jet
∞	free-stream conditions

Aerodynamic derivatives (referenced to a system of body axes):

$$C_{l_\beta} = \frac{\partial C_l}{\partial \beta} \qquad C_{n_\beta} = \frac{\partial C_n}{\partial \beta}$$

$$C_{l_{\delta_a}} = \frac{\partial C_l}{\partial \delta_a} \qquad C_{n_{\delta_a}} = \frac{\partial C_n}{\partial \delta_a}$$

$$C_{l_{\delta_r}} = \frac{\partial C_l}{\partial \delta_r} \qquad C_{n_{\delta_r}} = \frac{\partial C_n}{\partial \delta_r}$$

RESEARCH ROCKET SYSTEM

A rocket system was designed for relatively easy installation in a light airplane with minimal structural modification to the airplane. A pressurization and control unit was located in place of the right front seat of the plane and thrusters were appropriately oriented on the wing tips. The design goal was to produce a system weighing approximately the same as the weight of a seat plus a passenger. The arrangement of rocket system and data system components installed on the test airplane is presented in figure 1. A summary of the test airplane characteristics is presented in table I.

A hydrogen peroxide system was chosen because of the considerable experience with such systems at the Langley Research Center and the availability of existing components. A summary of the use of concentrated hydrogen peroxide as a fuel is presented in reference 5.

The sizing of the thrusters was based principally on estimates of the yawing acceleration required for spin recovery, inasmuch as the system was intended to be used ultimately in spin recovery studies, and it was desired to have sufficient torque about the yaw body axis to insure satisfactory recovery. A survey of pertinent spin-tunnel reports, such as reference 6, indicated that an acceleration of 1.0 rad/sec^2 would be more than adequate to provide rapid recovery for a wide range of yaw inertias; consequently, this value was selected as a design criterion. For the dimensions and estimated yaw inertia of the airplane, a rocket located at the wing tip would require a thrust of

620 N (140 lbf) to produce the design criterion. This amount of thrust was expected to be provided by using two thrusters for each wing-tip installation.

Another parameter required in sizing of the tanks for the rocket system was firing time. A value of 60 seconds of total firing time per fuel load was chosen to provide the possibility of several spin recovery attempts in one flight. This value dictated that for the size of thrusters used, about 23 kg (50 lbm) of fuel need to be carried in the fuel tanks.

A view of the airplane in flight with the rocket system installed is shown in figure 2. In this view the rockets are oriented to produce an unbalanced yawing moment. The thrusters are fired on only one wing tip at a time and thus produce a net forward thrust on the airplane. The boom near each wing tip is part of the instrumentation system that will be discussed subsequently. The rocket system is shown schematically in figure 3 and system characteristics are presented in table II. Concentrated hydrogen peroxide (used as a monopropellant) is decomposed under pressure in the presence of a silver screen catalyst in the rocket motor to yield a gaseous mixture of oxygen and superheated steam. The gas is expanded through a convergent-divergent nozzle to produce thrust. Pressurization of the fuel system is provided by gaseous nitrogen stored at high pressure. A ground adjustable regulator reduces and regulates the pressure to a lower "system pressure" which expels the hydrogen peroxide from bladder-type storage tanks. Bladder tanks were used to insure flow from the tanks for all flight conditions such as large attitudes. Fuel is fed through tubes in the wing to electrically controlled solenoids at each wing tip which control the flow of fuel to the motors in an on-off manner. Spring-type relief valves in the nitrogen systems and redundant rupture disks in the hydrogen peroxide system provide protection from overpressure. Fuel system pressure, set by the pressure regulator, determines the thrust of the motors.

The rocket motors (two on each wing tip) shown in figures 4 and 5 are attached normal to a tubular strut (mounted normal to the wing tip rib) which can be rotated 360°. The motor assembly, with appropriately installed tubing, can be rotated to provide yawing moments (fig. 4), rolling moments (fig. 5), or continuous combinations thereof. It should be pointed out that when the motor nozzles are oriented downward to provide a rolling moment, the thrust axis is canted outward at an angle equal to the dihedral of the wing (6.5°). Although one properly sized motor could have been used on each wing tip to provide the required thrust, two motors were used because of the availability. The thrusters are usually not oriented to fire forward because of the exhaust being blown back over the wing. Thus, yawing moments are always coupled with forward thrust. When oriented for roll, the thrusters are also only fired on one wing tip at a time, so that rolling moments are accompanied by vertical thrust.

Hydrogen peroxide is an extremely active oxidizing agent which should not come in contact with many materials, including human skin. The system is, therefore, enclosed by an aluminum box attached to the right, front-seat rails (fig. 6). The enclosure is leakproof and fume-tight (within the cabin) with a vent on the right door for servicing. Pressure vent and enclosure drain lines are routed overboard through the cockpit floor.

All tubing is stainless steel and the fittings outside the enclosure are available for inspection. The tubing from the cockpit to the wing tip is one piece to preclude an undetectable leak. Because of the long run of tubing to the wing tip, it was necessary to install a standpipe at the wing tip to minimize the reflected pressure wave (water hammer) that occurred each time the solenoid valve was closed.

Aside from the safety provided by adequate structural margins and overboard vents, there are some operational factors which the pilot can control that contribute to the safety of the system. In the event a solenoid fails to close, resulting in a "stuck thruster," there is a three-way valve which can be controlled by the pilot with a handle located on top of the enclosure that will vent the pressurized hydrogen peroxide from the motors. Furthermore, the pilot can deplete the complete fuel supply in approximately 45 seconds by firing both sets of motors at once. In the event of loss of electric power to the solenoids, a hand-operated valve on top of the enclosure will allow the pilot to bleed the fuel out of the bottom drain. Spring-loaded off (push button) firing switches are located on the pilot's control wheel (fig. 7) oriented right and left for right and left yaw and for right and left roll, depending on the orientation of the motors. Another switch is provided for firing both sets of motors at the same time.

A service cart was constructed for transferring hydrogen peroxide and nitrogen from storage facilities and for servicing the rocket system. There was sufficient hydrogen peroxide and nitrogen on the cart for three fuelings.

DATA ACQUISITION

An analog data collection system that combines the techniques of frequency modulation (FM) and sampled pulse amplitude modulation (PAM) was installed in the airplane. Data were recorded on magnetic tape by the direct recording method. A description of similar systems is presented in reference 6. There are 20 channels of continuous FM data and 28 channels of time-shared PAM data. The time-shared data were sampled with a 600 sample per second commutator that can sample each of 30 signals, 20 times per second.

Measurements

Transducers located about the airplane provide a measure of pilot inputs and resulting airplane dynamics. A measurement list is presented in table III.

True airspeed, angle of attack, and angle of sideslip are determined from a swiveling anemometer mounted on booms ahead of each wing tip (fig. 8). The use of a similar anemometer to measure airspeed is described in reference 7. In addition to true airspeed measurements, indicated airspeed was obtained from the airplane's system, which consists of a simple total-pressure probe mounted under the left wing tip and flush static-pressure orifices on both sides of the aft fuselage. Total temperature was measured by a sensor located on the top of the fuselage just aft of the passenger compartment.

A triad of linear accelerometers is rigidly mounted on the center line of the cockpit floor at a location approximately in the center of the allowable center-of-gravity range of the airplane. Aerodynamic control surface motions (ailerons, rudder, stabilator, and flaps) are measured by rotary potentiometers attached directly to the surface in question. One absolute pressure transducer is mounted inside each wing tip thruster unit to measure the chamber pressure of one of the rockets for determination of thrust.

Other instrumentation, including rate gyros, attitude gyros, signal conditioning, power supplies, and tape recorder, is located on a two-tier rack located behind the front seats as shown in figure 9. The power is obtained from the airplane's 12-volt dc, 60-ampere alternator.

Data Reduction

The analog flight tape was digitized onto two tapes, one for continuous FM and one for sampled PAM, using an analog-to-digital transcriber (ADTRAN). The continuous data were filtered with a 6-Hz constant delay filter and sampled 20 times per second. The commutated data tape is essentially unfiltered and has the same sample rate at which it was recorded (20 times per second). The two digitized tapes were converted to engineering units and merged. This merged tape was used to obtain data tabulations and time history plots.

Thrust Calibrations

The rocket motors used in this program were equipped with convergent-divergent nozzles designed for complete expansion at standard sea-level conditions. The motors were also equipped with pressure taps in the decomposition chambers which were located immediately upstream of the nozzles. Each motor was calibrated in a ground test facility at standard sea-level conditions for thrust as a function of the chamber pressure. (See fig. 10.)

For this program one pressure transducer was mounted on each wing-tip rocket pod to measure the chamber pressure of one of the rockets in each pod. For single rocket motor operations the pressure transducers were attached to the active motors. For dual rocket motor operations (two thrusters fired together in a unit on each wing tip) the transducers were alternated between motors for each flight test. A ground calibration was made to determine the chamber pressure relationship between rocket motors in each unit. It was assumed that this relationship would remain constant; therefore, the chamber pressure of the unmeasured motors would be known.

The nominal test altitude for this program was 760 m (2500 ft). The correction for ambient pressure less than sea level was calculated to be a 1-percent increase in thrust for each 760 meters pressure altitude above sea level. (See ref. 8.) Since this correction was relatively small, it was not deemed necessary.

Flight Calibrations

A few of the measured quantities required calibration because of the location of the respective sensors in the flow field of the airplane. These quantities are airspeed, altitude, angle of attack, and angle of sideslip. The airspeed sensors, the airplane's airspeed system, and the altimeter were calibrated by using the trailing anemometer described in reference 9. The flight-test procedure used the stabilized point concept, and this method and appropriate equations are discussed in reference 9. For convenience, the indicated airspeed system of the airplane was used for determining airspeed and dynamic pressure. The calibration of the airspeed system is presented in figure 11 in terms of the static-pressure error coefficient $\Delta p/q_c$ as a function of indicated airspeed. The calibration was performed for the four flap positions obtainable and the results indicated that the flaps had little effect on the airspeed measurement. The angle of sideslip was obtained by averaging the readings of the vanes on the left and right wing-tip booms. No corrections for unsymmetrical in-flow at the wing tips due to sideslip were considered necessary (ref. 10). The true airspeed sensor calibration and angle-of-attack calibrations were obtained but are not presented in this report.

Test Technique and Analysis

Determination of rudder control effectiveness $C_{n_{\delta_r}}$ and aileron control effectiveness $C_{l_{\delta_a}}$ was based on equations that show the balance of moments in yaw and in roll with rockets on and rockets off. Simplified versions of the equations follow.

Rudder control effectiveness $C_{n_{\delta_r}}$.- The yawing-moment equation for wings-level trimmed flight at constant airspeed is as follows:

$$C_{n_{\delta_r}}\delta_{r,0} + C_{n_{\delta_a}}\delta_{a,0} + C_{n_\beta}\beta_0 = 0 \tag{1}$$

Yawing moment for wings-level trimmed flight with yaw rockets firing at the same airspeed is

$$\frac{M_{Z,R}}{qSb} + C_{n_{\delta_r}}\delta_{r,1} + C_{n_{\delta_a}}\delta_{a,1} + C_{n_\beta}\beta_1 = 0 \tag{2}$$

Combining equations (1) and (2) and collecting terms yields the following expression:

$$\frac{M_{Z,R}}{qSb} + C_{n_{\delta_r}}\left(\delta_{r,1} - \delta_{r,0}\right) + C_{n_\beta}\left(\beta_1 - \beta_0\right) + C_{n_{\delta_a}}\left(\delta_{a,1} - \delta_{a,0}\right) = 0 \qquad (3)$$

By performing the flight tests with and without the rockets firing so that $\delta_{a,1} = \delta_{a,0}$ and $\beta_1 = \beta_0$, equation (3) simplifies to

$$C_{n_{\delta_r}} = -\frac{M_{Z,R}/qSb}{\delta_{r,1} - \delta_{r,0}} = -\frac{M_{Z,R}/qSb}{\Delta\delta_{r,1}} \qquad (4)$$

The manuever used to obtain the measurements for determining $C_{n_{\delta_r}}$ is illustrated in figure 12 with the time histories of pertinent parameters. The pilot trimmed wings level, at an airspeed of approximately 63 knots while attempting to maintain constant altitude. He zeroed the ball in the "needle-ball indicator" to attain zero lateral acceleration and noted the value of sideslip angle β on the sideslip indicator. Subsequently, he fired the rockets on the right wing tip, as indicated by the rapid rise in rocket chamber pressure, and simultaneously applied almost full right rudder. (The noise in the chamber pressure measurement before and after firing is due to the data system extraneously picking up the signal from the pilot's radio transmitter.) The pilot's task was to maintain constant values of sideslip angle, heading, and airspeed (dynamic pressure) during the motor firing. The trim value of β, which the pilot previously noted, was the value he was attempting to hold. An initial transient in sideslip angle, aileron deflection, roll angle, and airspeed occurred when the rocket motors were fired. During this typical run the variation of airspeed was less than 2 knots; sideslip angle variation, less than 1°; and aileron deflection variation, less than 2°. The variations in these flight parameters during the rocket firing would produce an error in $C_{n_{\delta_r}}$ of approximately 0.008, using the values of C_{n_β} and $C_{n_{\delta_a}}$ found in reference 11.

Maneuvers were performed by firing the rockets on the right wing or on the left wing and were spot checked at a lower thrust level to determine any differences. Similar maneuvers were performed in a sawtooth climb (steady climbs at maximum power and steady descents at minimum power with constant airspeed) at a number of airspeeds to study power effects.

Aileron control effectiveness $C_{l_{\delta_a}}$.- The rolling-moment equation for wings-level trimmed flight at constant airspeed is

$$C_{l\delta_a}\delta_{a,0} + C_{l\delta_r}\delta_{r,0} + C_{l\beta}\beta_0 = 0 \tag{5}$$

The rolling-moment equation for wings-level trimmed flight with roll rockets firing (rocket moment balanced by the aileron) is

$$\frac{M_{X,R}}{qSb} + C_{l\delta_a}\delta_{a,1} + C_{l\delta_r}\delta_{r,1} + C_{l\beta}\beta_1 = 0 \tag{6}$$

Combining equations (5) and (6) and collecting terms yields the following expression:

$$\frac{M_{X,R}}{qSb} + C_{l\delta_a}\left(\delta_{a,1} - \delta_{a,0}\right) + C_{l\delta_r}\left(\delta_{r,1} - \delta_{r,0}\right) + C_{l\beta}\left(\beta_1 - \beta_0\right) = 0 \tag{7}$$

By performing flight tests similar to the yaw maneuvers such that $\delta_{r,1} = \delta_{r,0}$ and $\beta_1 = \beta_0$, equation (7) simplifies to

$$C_{l\delta_a} = -\frac{M_{X,R}/qSb}{\delta_{a,1} - \delta_{a,0}} \tag{8}$$

The maneuver used to obtain the measurements for determining $C_{l\delta_a}$ is illustrated by the time histories of pertinent parameters in figure 13. The pilot's task was to fire the roll rockets and deflect the ailerons simultaneously to hold the wings level while keeping changes in airspeed and sideslip to a minimum. The pilot held conditions reasonably constant in the maneuver. Of those parameters desired to be unchanged, the airspeed decreased approximately 3 knots, sideslip deviated less than 1°, and rudder deflection varied less than 1°. The variation in these flight parameters during the rocket firing would produce an error in $C_{l\delta_a}$ of about 0.026 by using values of $C_{l\delta_r}$ and $C_{l\beta}$ found in reference 11.

Test Conditions

Flight maneuvers were performed in smooth air at a nominal altitude of 760 m (2500 ft), except on a few occasions when it was necessary to operate at about 1500 m (5000 ft) to find smooth air. The tests were performed at calibrated airspeeds from 70 to 100 knots. It would have been desirable, from a stall/spin interest or point of view, to operate at airspeeds down to and below the stall speed. Testing was not performed at these low airspeeds

because the rocket system had not been demonstrated as a reliable spin recovery system and the planned installation of a spin recovery parachute had not been made. All flight tests were performed without flaps at a nominal mass of 1060 kg (2340 lbm). The center of gravity was located at 18 percent of the mean aerodynamic chord.

RESULTS AND DISCUSSION

In this section first the operational experience with the rocket system is discussed and then the results of rudder and aileron effectiveness measurements for airspeeds above the stall are presented. Results of these control effectiveness measurements are compared with another flight-test technique and with readily available analytical techniques.

Operational Experience

Operational experience with the rocket system was obtained from a flight-test program of 15 flights with an accumulated rocket firing time of approximately 20 min. With the service facilities available, two flight operations per 8-hr day were readily accomplished. Turnaround time between flights for rocket system servicing was 1 hr.

The thrust nominally available at maximum fuel pressure was found to be 490 N (110 lbf). This thrust is about 21 percent below the design thrust level, probably because of excessive pressure drop in several system components. The loss, however, did not have any influence on the results of the particular tests covered in this report.

There was no accurate method of determining the remaining rocket fuel quantity in flight and, as a result, the remaining firing time was estimated by the ground crew, who were keeping an accumulated firing-time record from the on-off signals radioed by the pilot and from the knowledge of total firing time available for a full load of fuel.

Control Effectiveness

The rudder deflection required to balance the yawing moment produced by the rockets is presented as a function of calibrated airspeed for trimmed level flight (fig. 14). Power for level flight was used and the rockets were fired to produce both left and right yawing moments. The variation in rudder deflection for the trim conditions with the rockets off at zero lateral acceleration (since the "ball" was centered) shows the effect of the rotation of the slipstream and propeller yawing moment. Most of the data are for the condition of maximum nominal thrust of 490 N (110 lbf), which produced a moment of 2500 N-m (1840 ft-lbf), with a few points for the minimum nominal thrust condition of 250 N (60 lbf), which produced a moment of 1300 N-m (960 ft-lbf). The data indicate that for airspeeds approaching the stall (approximately 57 knots), the rudder deflection approaches the maximum available (25^{o}) for the maximum moment condition. The reduction of about one-half in rocket thrust appears to cut the

change in rudder deflection by a similar amount. The data for right and left rudder deflection indicate the possibility that rudder effectiveness for positive deflection (trailing edge left) is greater than that for negative deflection. This supposition arises from the fact that the change in rudder deflection required to balance the rocket yawing moment is greater in the case of the negative rudder deflection than in the case of the positive deflection.

Figure 15 compiles rudder deflection data, both for the power for level flight of the previous figure and for sawtooth climbs, and shows the change in rudder deflection as a function of calibrated airspeed in knots. All the data are for rocket firings utilizing the minimum (one-half) rocket-produced moment. This figure shows the effect of power, since the descents in the sawtooth climb maneuver were at idle power, and the climbs used maximum power. The general reduction in rudder deflection required to balance rocket moment as airspeed increased reflects the corresponding increase in dynamic pressure at the tail. Similarly, from the sawtooth climbs, the increase in power with a corresponding increase in dynamic pressure at the tail results in a decrease in rudder deflection required.

The values of $C_{n_{\delta_r}}$, as determined from these data of figures 14 and 15 and by equation (4), are presented in figure 16 as a functiuon of calibrated airspeed in knots. The large variations in rudder effectiveness at a given airspeed reflect the power effects shown by the corresponding rudder deflection data of figure 15.

In an effort to examine the results further, comparisons are presented (fig. 17) for an analytical estimation and other experimental measurement techniques for the level-flight trim condition. The ability of the pilot to hold desired test conditions, as indicated earlier, would produce an error in $C_{n_{\delta_r}}$ of 0.008, which is approximately 10 percent of the average rudder effectiveness presented in figure 17. The analytical estimation was made by use of the method suggested in reference 10. The additional experimental data were obtained from dynamic maneuvers for which the data were analyzed by using a modified maximum likelihood method of derivative extraction (ref. 12). This flight investigation was part of a continuing flight program at Langley Research Center to determine stability derivatives of light airplanes. (See ref. 11.) The agreement between the two experimental techniques is good, whereas the analytical estimation appears to be too high in magnitude.

The aileron deflection required to balance the rocket-produced rolling moment for two thrust levels is shown as a function of calibrated airspeed in figure 18. Also shown is the trim aileron position without the rockets firing. The aileron deflections required to balance the rocket-produced moments do not approach maximum (approximately 18°) even at the lowest airspeed.

The variation in $C_{l_{\delta_a}}$ as a function of calibrated airspeed is presented in figure 19. The ability of the pilot to hold desired test conditions, as indicated earlier, would produce an error in $C_{l_{\delta_a}}$ of 0.026, which is approxi-

mately 10 percent of the average aileron effectiveness presented in figure 19. Also shown for comparison are the experimental data from dynamic maneuvers obtained by using the maximum likelihood method of derivative extraction and the results of two analytical estimation techniques from references 13 and 14. The two experimental methods produced very similar results, whereas the analytical estimations are consistently lower than the measured values.

Effects of Rocket Operation on Control Effectiveness

Several influences on roll and yaw effectiveness are possible from the operation of wing-tip rockets. The principal effects are impingement of the rocket exhaust on the tail and changes in the wing-tip pressure distribution due to the interaction of the jet and the free stream. The significance of some of these influences are noted in reference 15 from wind-tunnel tests of a turbojet engine mounted on the wing tip of a transport airplane exhausting rearward and in reference 16, which shows measured losses in roll effectiveness resulting from rockets exhausting normal to the wing tip of a subsonic vertical take-off and landing (VTOL) model.

Some insight into the problem for the results reported herein was available from the "warm-up" phase of the firing operations. Hydrogen peroxide motors normally have an invisible exhaust; however, they characteristically do not realize complete decomposition of the fuel until the catalyst bed is warmed. There was, in this operation, a short period during the warm-up in which the exhaust products were largely visible steam. Movies of the firings were taken to study the action of the exhaust. Still photographs taken from these movies during the time steam was produced are presented in figure 20; these photographs indicate that the visible exhaust did not impinge on the tail.

In an effort to determine the flow interaction effects, an unpublished analytical study was performed based on a model of sink-source distribution along the rocket wake axis used in reference 17 combined with a vortex-lattice representation of the lifting surface. This analysis indicated a negligible change in both rudder and aileron effectiveness as a result of rocket operation. However, the results of reference 16 indicate that for the VTOL model a loss of 8 to 10 percent of the applied rolling moment occurred at the rocket velocity ratio $\sqrt{\rho_\infty V_\infty^2/\rho_j V_j^2}$ equal to that generated by the present rockets. The location of the jet on the VTOL model, for which the loss in rolling moment was quoted, was 10.1 cm (4 in.) inboard of the wing tip at 50 percent chord. The location of the present rocket, 15.2 cm (6 in.) outboard of the tip at 50 percent chord, would be expected to reduce this loss. The fairly good agreement of the rocket-generated aileron and rudder effectiveness data with the values obtained from the derivative extraction technique increases the confidence that the effects of the jet are small.

CONCLUDING REMARKS

A hydrogen-peroxide-fueled rocket system was installed on a light, four-place general aviation airplane to provide known moments about the roll and

yaw axes for use in measuring control effectiveness for all flight conditions. The system produced thrust up to approximately 490 N (110 lbf) with pilot-controlled firing time of about 60 seconds at this thrust level. Flight operations totaling 15 with approximately 20 minutes of accumulated firing time were accomplished without any hardware or operational problems.

A technique for measuring control effectiveness by using rocket-generated roll and yaw moments was developed. Rudder and aileron effectiveness $\left(C_{n_{\delta_r}}\right.$ and $\left.C_{l_{\delta_a}}\right)$ for airspeeds near stall to near cruise (approximately 65 to 100 knots) were measured by using this technique. These results agreed with results obtained from dynamic flight maneuvers that used the maximum likelihood method of stability extraction. Comparison of the measured derivatives with readily available estimation techniques indicated that the estimates for both derivatives differed appreciably from those measured.

Langley Research Center
National Aeronautics and Space Administration
Hampton, VA 23665
March 12, 1980

REFERENCES

1. Perkins, Courtland D., ed.: [AGARD] Flight Test Manual. Volume II - Stability and Control. Pergamon Press, 1963.

2. Burk, Sanger M., Jr.; and Healy, Frederick M.: Comparison of Model and Full-Scale Spin Recoveries Obtained by Use of Rockets. NACA TN 3068, 1954.

3. Farmer, G. H.; and Peterson, B. G.: Flight Test Investigation To Determine the Effectiveness of a Rocket as an Emergency Spin Recovery Device. Rep. No. NA-52-771 (Contract AF-33(038)-23809), North American Aviation, Inc., June 27, 1952.

4. Mechtly, E. A.: The International System of Units - Physical Constants and Conversion Factors (Second Revision). NASA SP-7012, 1973.

5. Handbook - Field Handling of Concentrated Hydrogen Peroxide (Over 52 Weight Percent Hydrogen Peroxide). NAVAER 06-25-501, Bur. Aero., July 1, 1955. (Rev. Jan. 15, 1957.)

6. Pool, A.; and Bosman, D., eds.: Basic Principles of Flight Test Instrumentation Engineering. AGARD-AG-160-VOL 1, 1974.

7. Kershner, David D.: A Suspended Anemometer System for Measuring True Airspeed on Low-Speed Airplanes. NASA TN D-8523, 1977.

8. Sutton, George P.: Rocket Propulsion Elements. John Wiley & Sons, Inc., 1949.

9. Fisher, Bruce D.; Holmes, Bruce J.; and Stough, H. Paul, III: A Flight Evaluation of a Trailing Anemometer for Low-Speed Calibrations of Airspeed Systems on Research Aircraft. NASA TP-1135, 1978.

10. McFadden, Norman M.; Rathert, George A., Jr.; and Bray, Richard S.: Flight Calibration of Angle-of-Attack and Sideslip Detectors on the Fuselage of a 35°_{3} Swept-Wing Fighter Airplane. NACA RM A52A04, 1952.

11. Klein, Vladislav: Determination of Stability and Control Parameters of a Light Airplane From Flight Data Using Two Estimation Methods. NASA TP-1306, 1979.

12. Grove, Randall D.; Bowles, Roland L.; and Mayhew, Stanley C.: A Procedure for Estimating Stability and Control Parameters From Flight Test Data by Using Maximum Likelihood Methods Employing a Real-Time Digital System. NASA TN D-6735, 1972.

13. Smetana, Frederick O.; Summey, Delbert C.; and Johnson, W. Donald: Riding and Handling Qualities of Light Aircraft - A Review and Analysis. NASA CR-1975, 1972.

14. USAF Stability and Control Datcom. Contracts AF 33(616)-6460 and F33615-75-C-3067, McDonnell Douglas Corp., Oct. 1960. (Revised Apr. 1976.)

15. Patterson, James C., Jr.; and Flechner, Stuart G.: An Exploratory Wind-Tunnel Investigation of the Wake Effect of a Panel Tip-Mounted Fan-Jet Engine on the Lift-Induced Vortex. NASA TN D-5729, 1970.

16. Spreemann, Kenneth P.: Free-Stream Interference Effects on Effectiveness of Control Jets Near the Wing Tip of a VTOL Aircraft Model. NASA TN D-4084, 1967.

17. Putnam, Lawrence E.: An Analytical Study of the Effects of Jets Located More Than One Jet Diameter Above a Wing at Subsonic Speeds. NASA TN D-7754, 1974.

TABLE I.- AIRPLANE CHARACTERISTICS

Maximum gross mass (normal category), kg (lbm)	1110 (2450)
Maximum gross mass (aerobatic category), kg (lbm)	930 (2050)
Engine, kW (hp)	130 (180)
Propeller diameter, m (ft)	1.9 (6.3)
Propeller activity factor	92
Wing airfoil	NACA 63_2A415
Wing span, m (ft)	10 (33)
Wing area, m^2 (ft^2)	13.6 (146)
Wing chord, m (ft)	1.34 (4.4)
Wing mean aerodynamic chord, m (ft)	1.34 (4.4)
Aspect ratio	7.34
Dihedral, deg	6.5
Aileron span, m (ft)	1.6 (5.4)
Aileron area (each), m^2 (ft^2)	0.47 (5.06)
Aileron chord, m (ft)	0.39 (1.3)
Vertical-tail airfoil	NACA 63_1A012 modified
Vertical-tail area, m^2 (ft^2)	1.36 (14.6)
Rudder area, m^2 (ft^2)	0.43 (4.62)
Horizontal-tail airfoil	NACA 63_1A012 modified
Horizontal-tail area, m^2 (ft^2)	2.51 (27.0)
Tail length (quarter chord of wing to quarter chord of vertical tail), m (ft)	4.14 (13.6)

TABLE II.- ROCKET SYSTEM CHARACTERISTICS

Fuel	Hydrogen peroxide (90% concentration by weight)
Fuel quantity, kg (lbm)	23 (50)
Pressurizing agent	Gaseous nitrogen
System mass:	
Pressurization unit in cockpit, kg (lbm)	52.2 (115)
Fuel, kg (lbm)	23 (50)
N_2, kg (lbm)	0.45 (1)
Rocket assembly (total of 2), kg (lbm)	14 (30)
Wing tip reinforcement (both tips), kg (lbm)	2.3 (5)
Supply tubing, kg (lbm)	3.2 (7)
Total, kg (lbm)	94.3 (208)
System performance:	
Maximum thrust (2 motors), N (lbf)	490 (110)
Minimum thrust (1 motor), N (lbf)	250 (57)
Firing time, sec:	
Thrust of 490 N (110 lbf)	60
Thrust of 250 N (57 lbf)	75

TABLE III.- MEASUREMENT LIST

Measurement	Range
Airspeed (pressure), kPa (psid)	0 to 3500 (0 to 0.5)
Airspeed (right and left), m/sec (ft/sec)	21 to 61 (70 to 200)
Angle of attack (right and left), deg	±100 or (0 to 30)
Angle of sideslip (right and left), deg	±55 or (±25)
Altitude, m (ft)	-152 to 2900 (-500 to 9500)
Normal acceleration, g units	-3 to 6
Lateral acceleration, g units	±1
Longitudinal acceleration, g units	±1
Pitch rate, deg/sec	±100
Roll rate, deg/sec	±270
Yaw rate, deg/sec	±270
Pitch attitude, deg	±80
Roll attitude, deg	±175
Yaw attitude, deg	±175
Stabilator deflector, deg	-16 to 3
Aileron deflection (right and left), deg	-24 to 10
Rudder deflection, deg	±30
Trim tab deflection, deg	-18 to 13
Flap deflection, deg	0 to 35
Throttle, percent	0 to 100
Longitudinal wheel force, N (lbf)	±445 (±100)
Lateral wheel force, N (lbf)	±156 (±35)
Rudder pedals force, N (lbf)	±445 (±100)
Engine speed, rpm	0 to 2900
Rocket chamber pressure (right and left), MPa (psia)	0 to 2 (0 to 300)
Rate of climb, m/sec (ft/min)	±13 (±2500)
Total temperature, ^{o}C (^{o}F)	-18 to 38 (0 to 100)

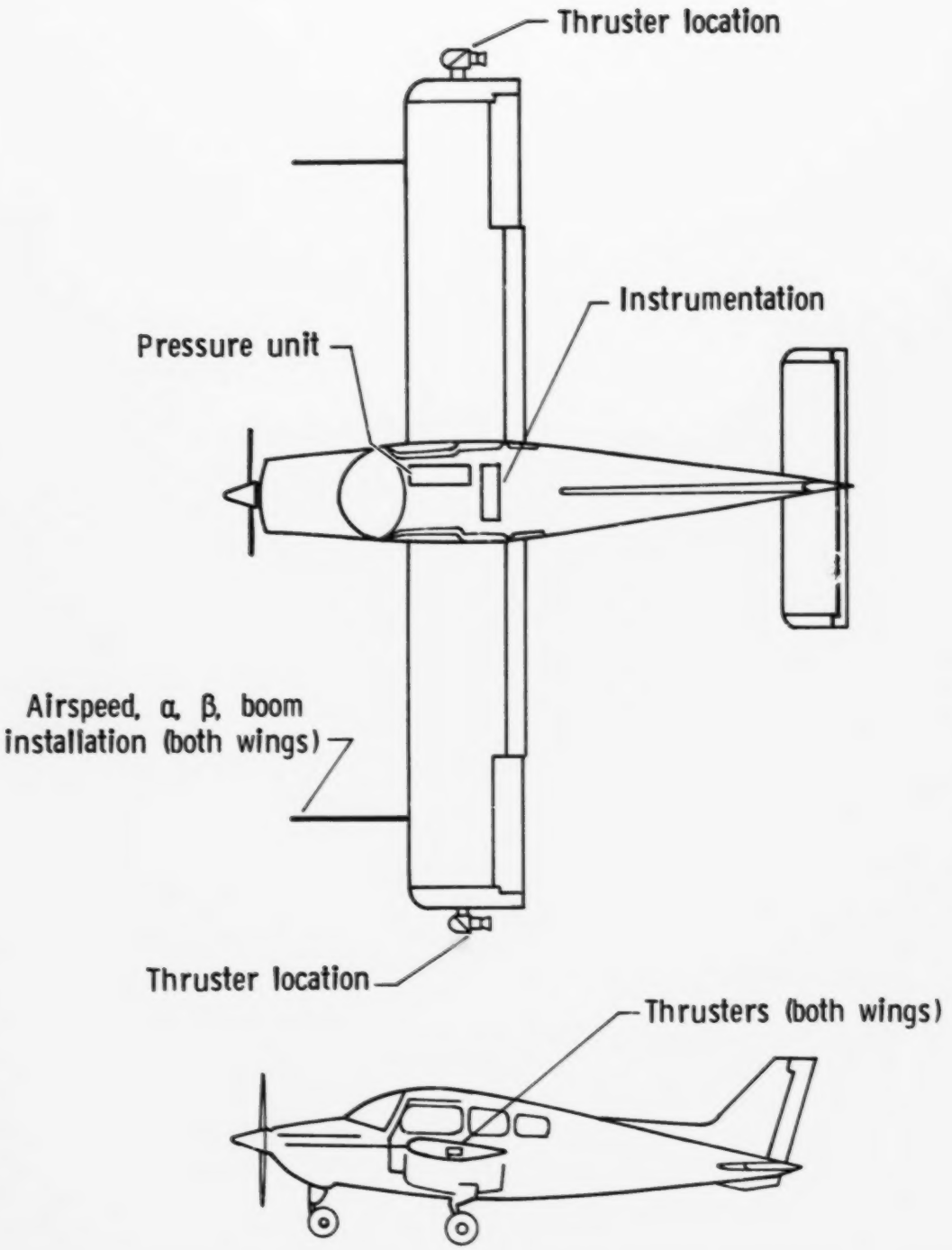

Figure 1.- Arrangement of rocket system and data system components installed on test airplane. Thrusters shown are oriented for yaw.

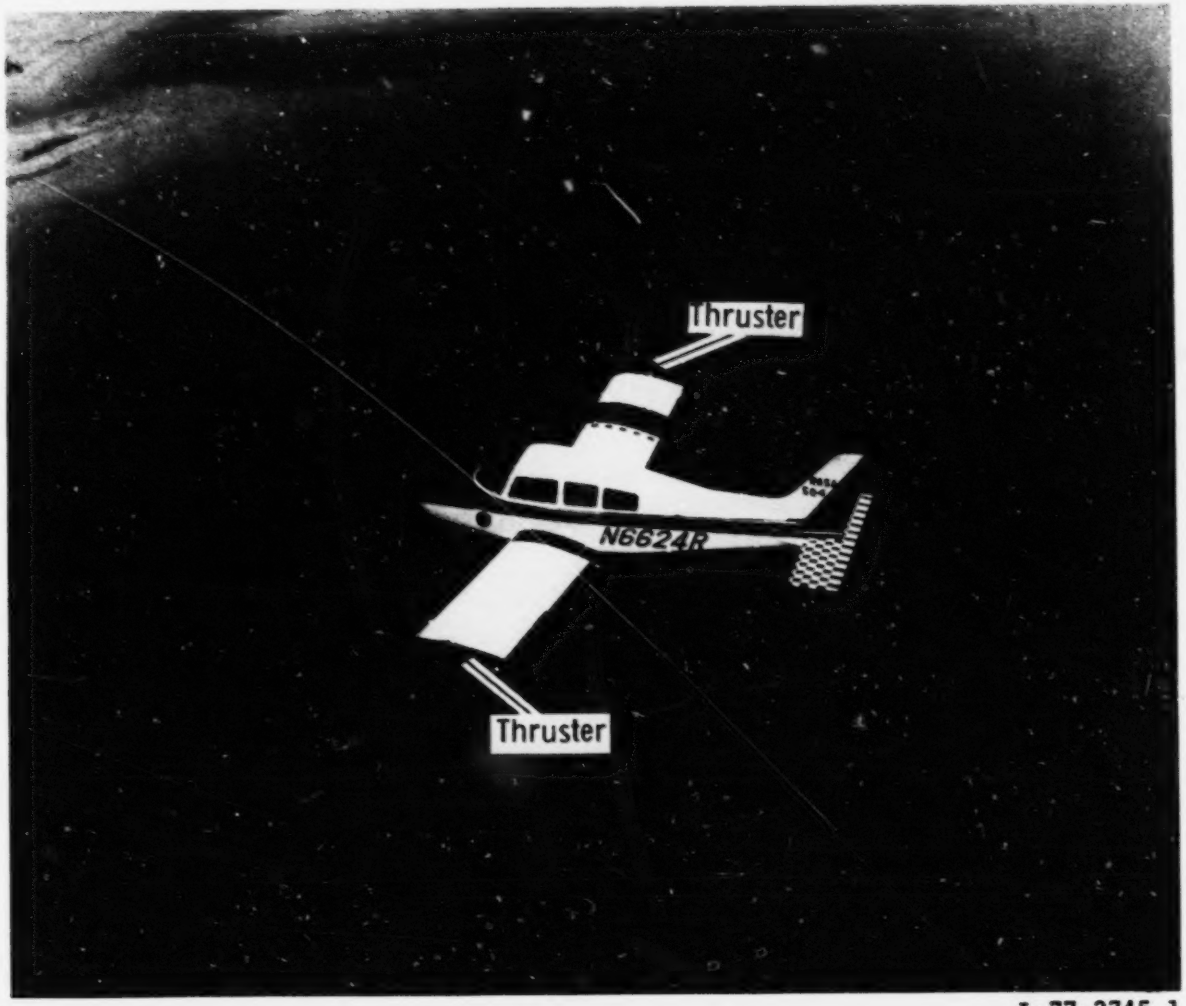

L-77-2745.1

Figure 2.- Airplane in flight with rocket system installed.

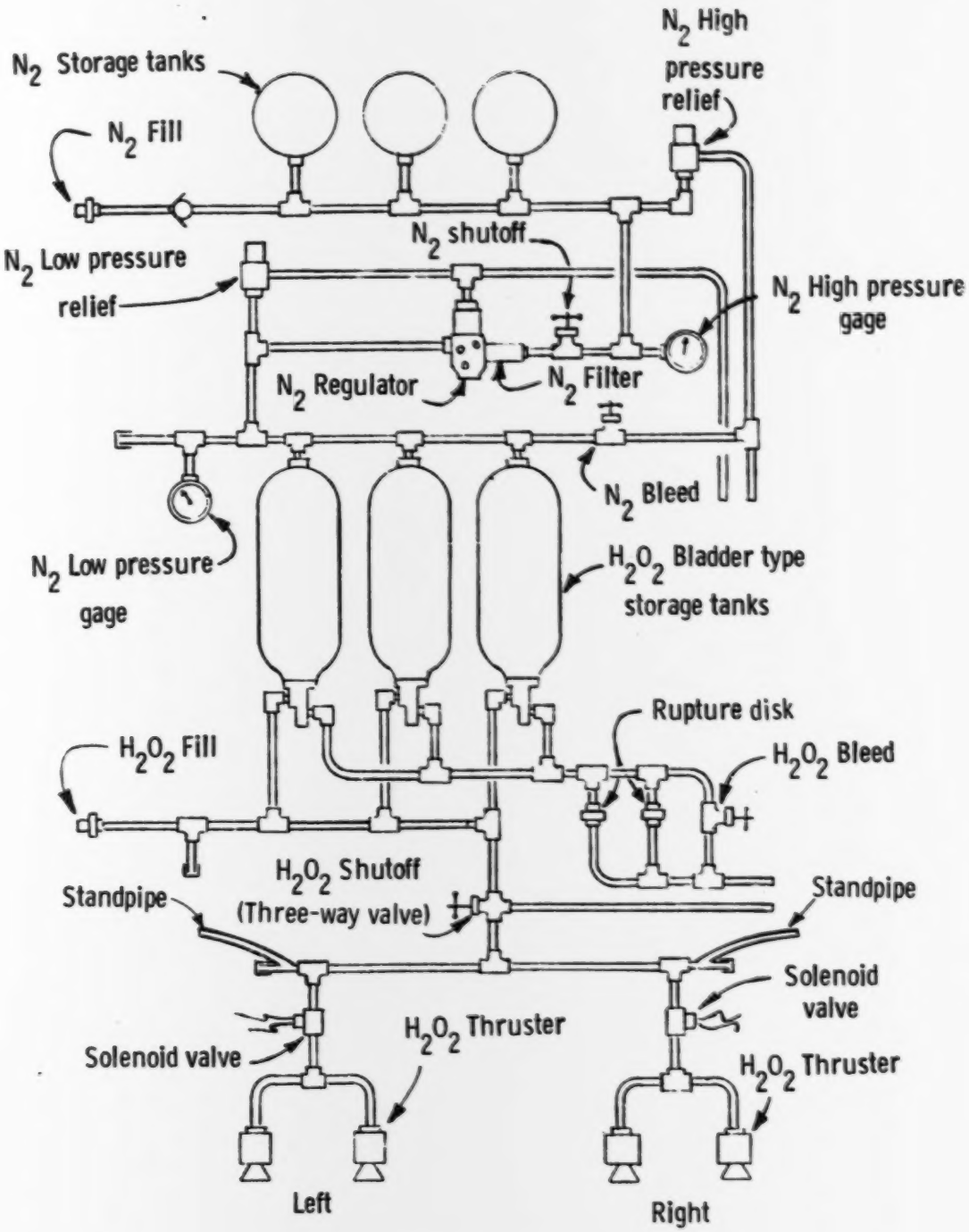

Figure 3.- Schematic of rocket system.

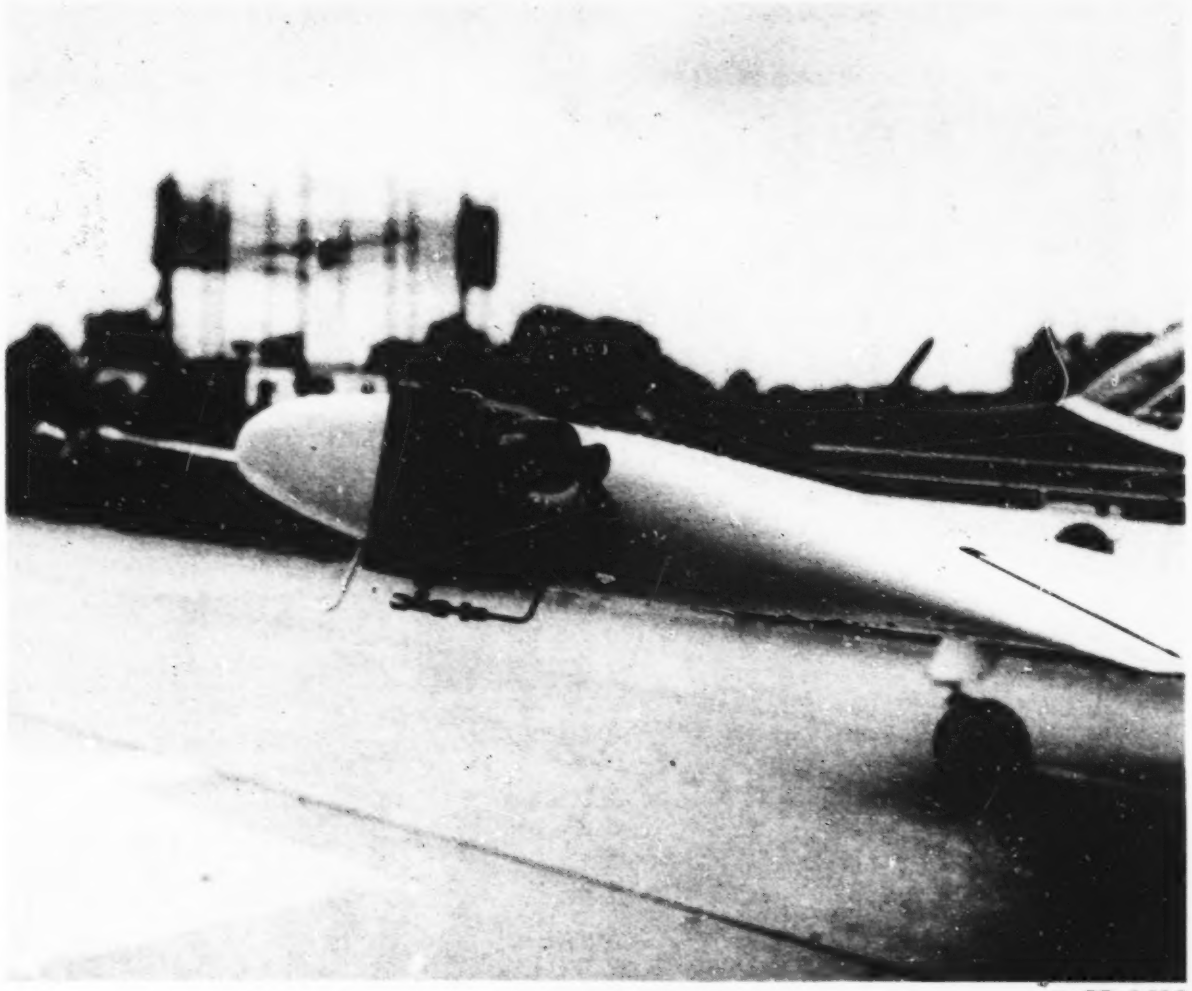

L-77-3606

Figure 4.- Rocket thrusters aligned to produce yawing moment.

BLANK PAGE

BLANK PAGE

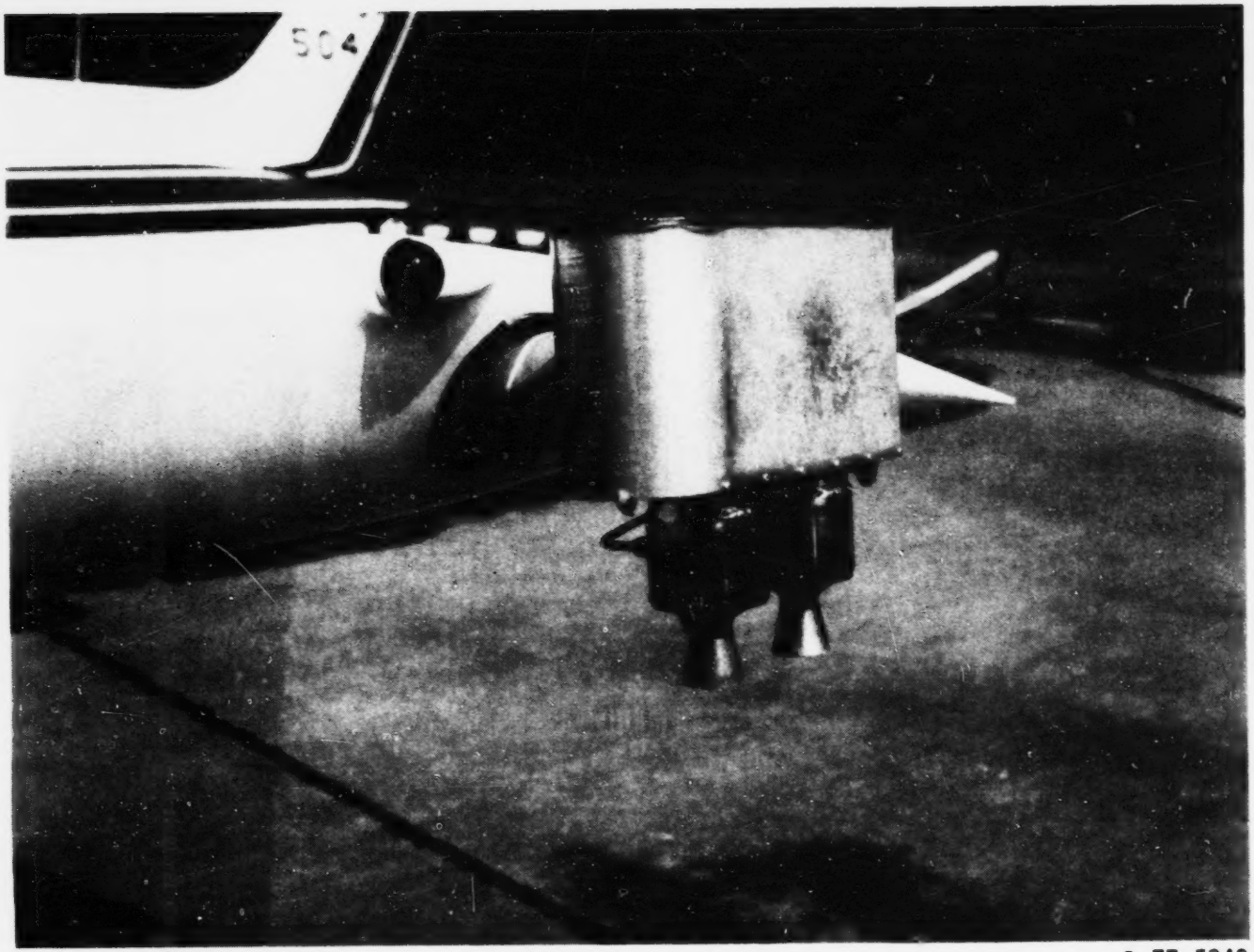

L-77-5249

Figure 5.- Rocket thrusters aligned to produce rolling moment.

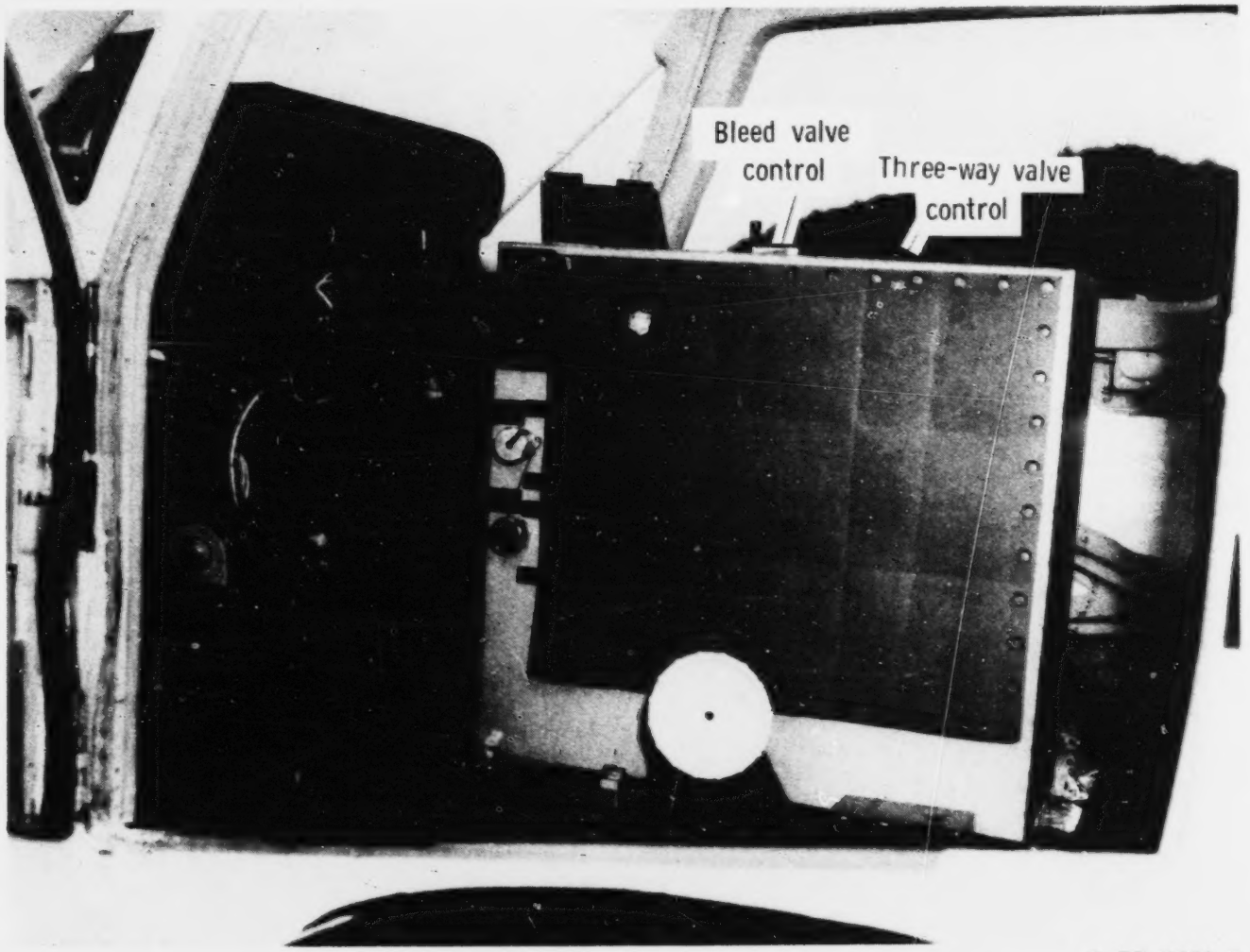

L-77-3608.1

Figure 6.- Pressurization system installed on right front-seat rails.

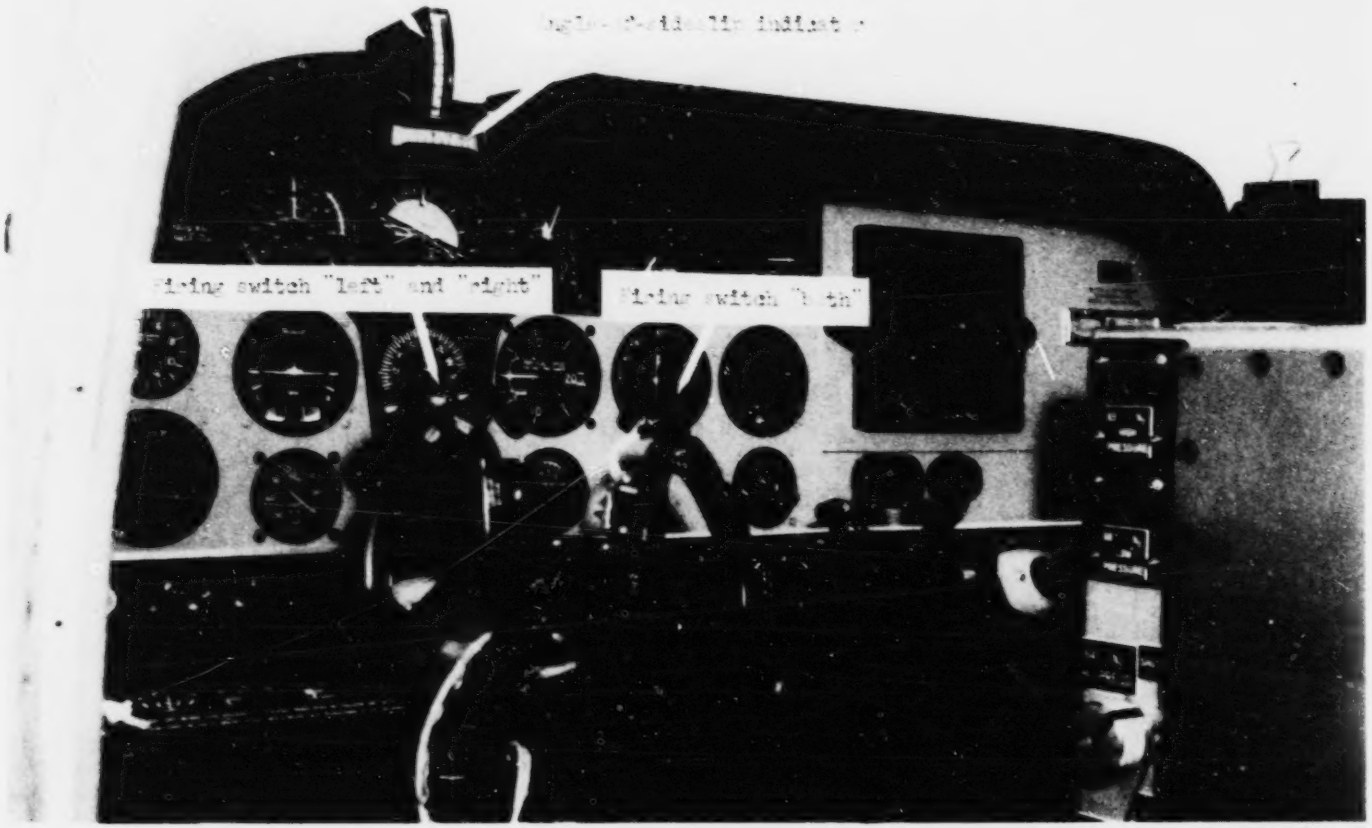

L-77-3609.1

Figure 7.- Arrangement of pilot controls and displays for performing rocket-firing data runs.

L-76-6604

Figure 8.- True airspeed, angle-of-attack, and angle-of-sideslip transducer.

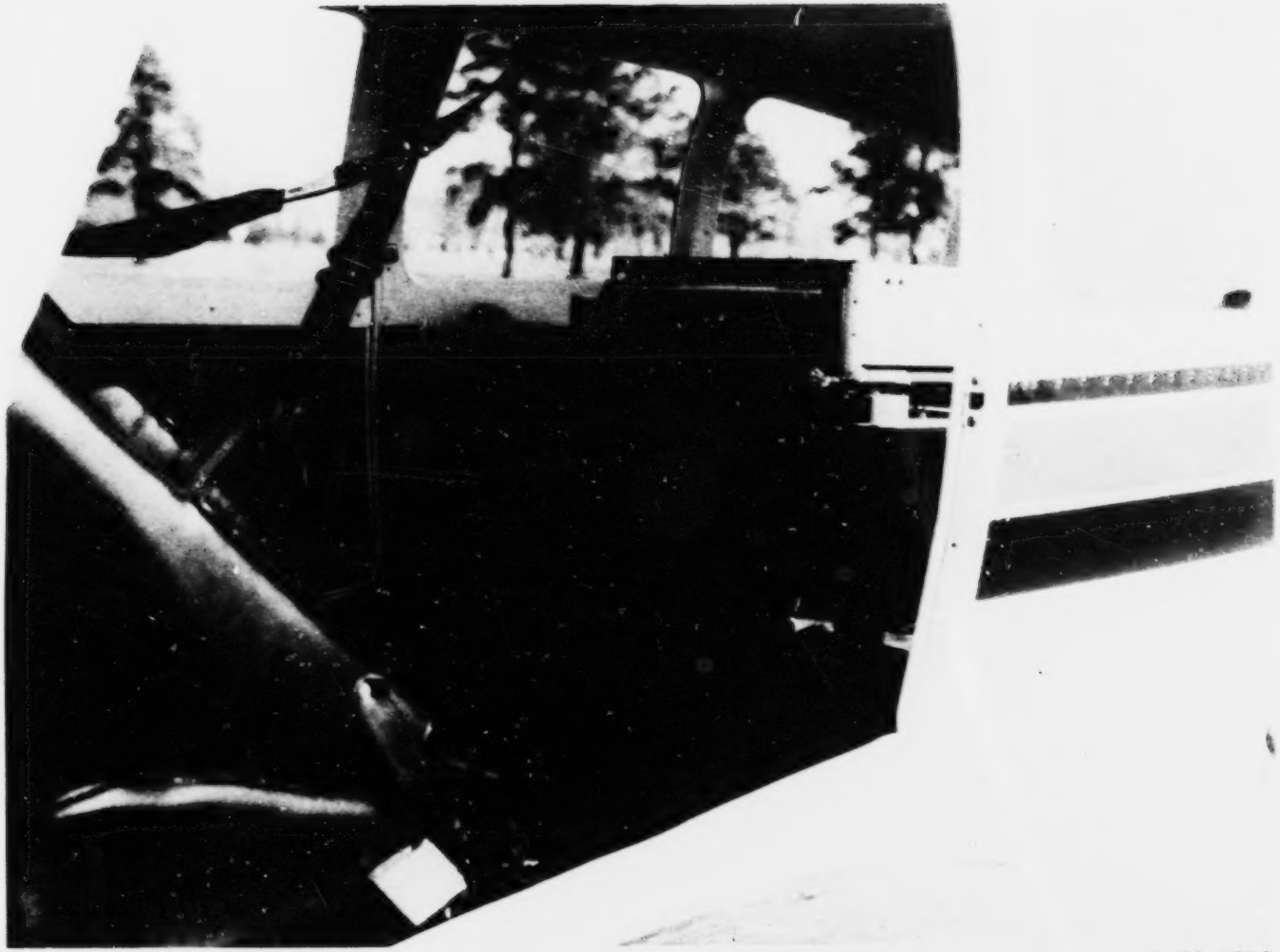

L-76-1812

Figure 9.- Instrumentation rack installed in airplane.

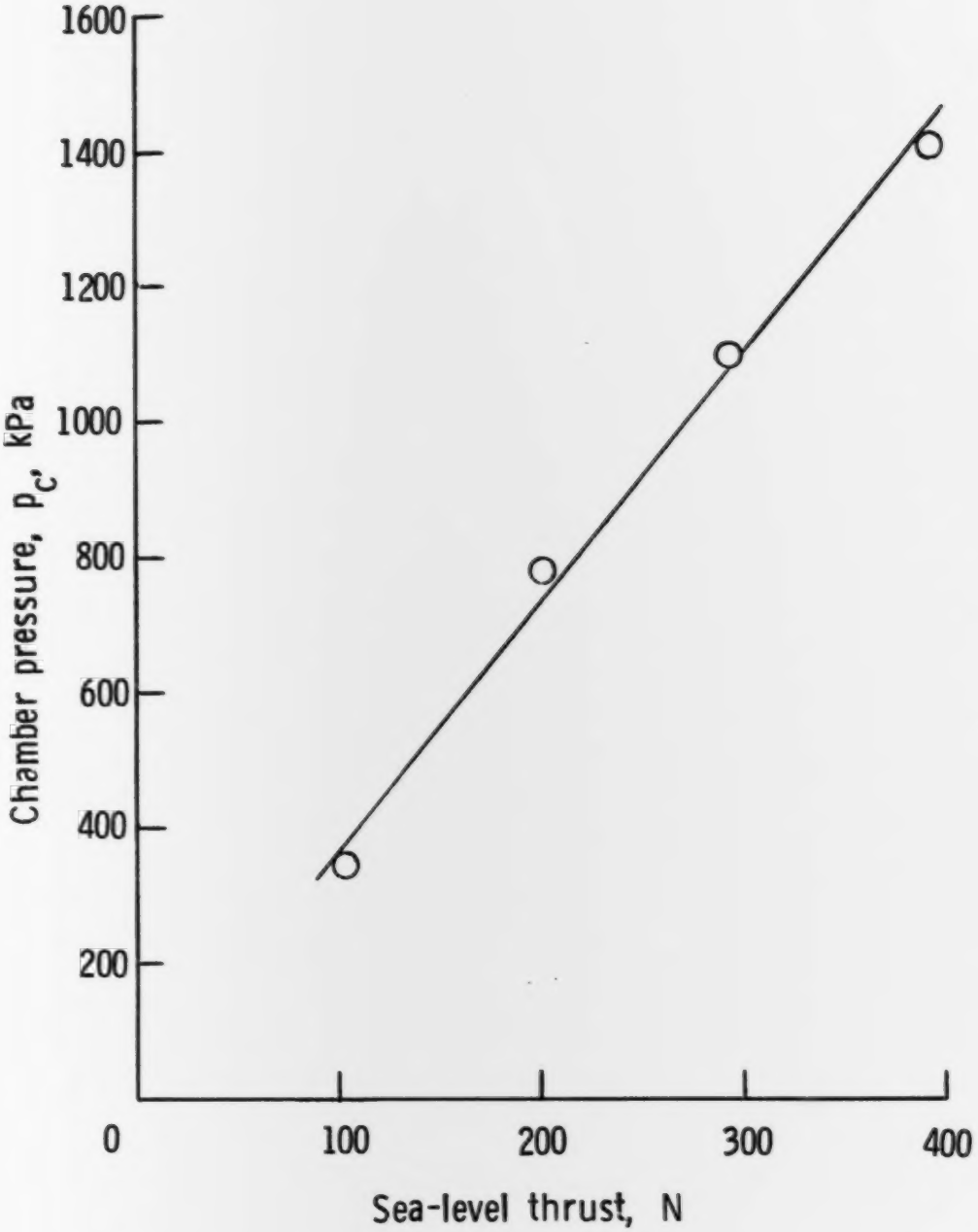

Figure 10.- Typical thruster sea-level calibration.

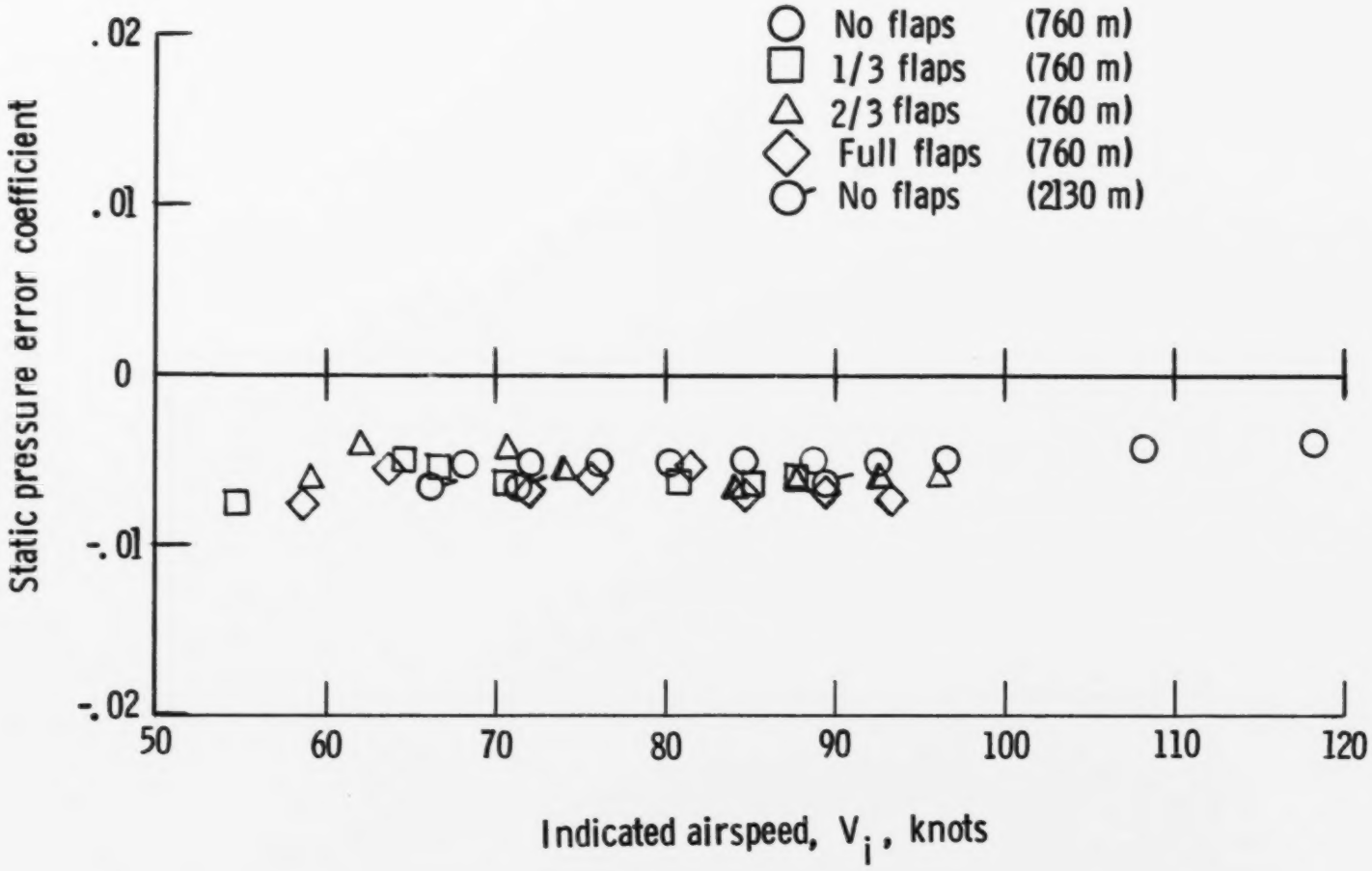

Figure 11.- Airspeed calibration.

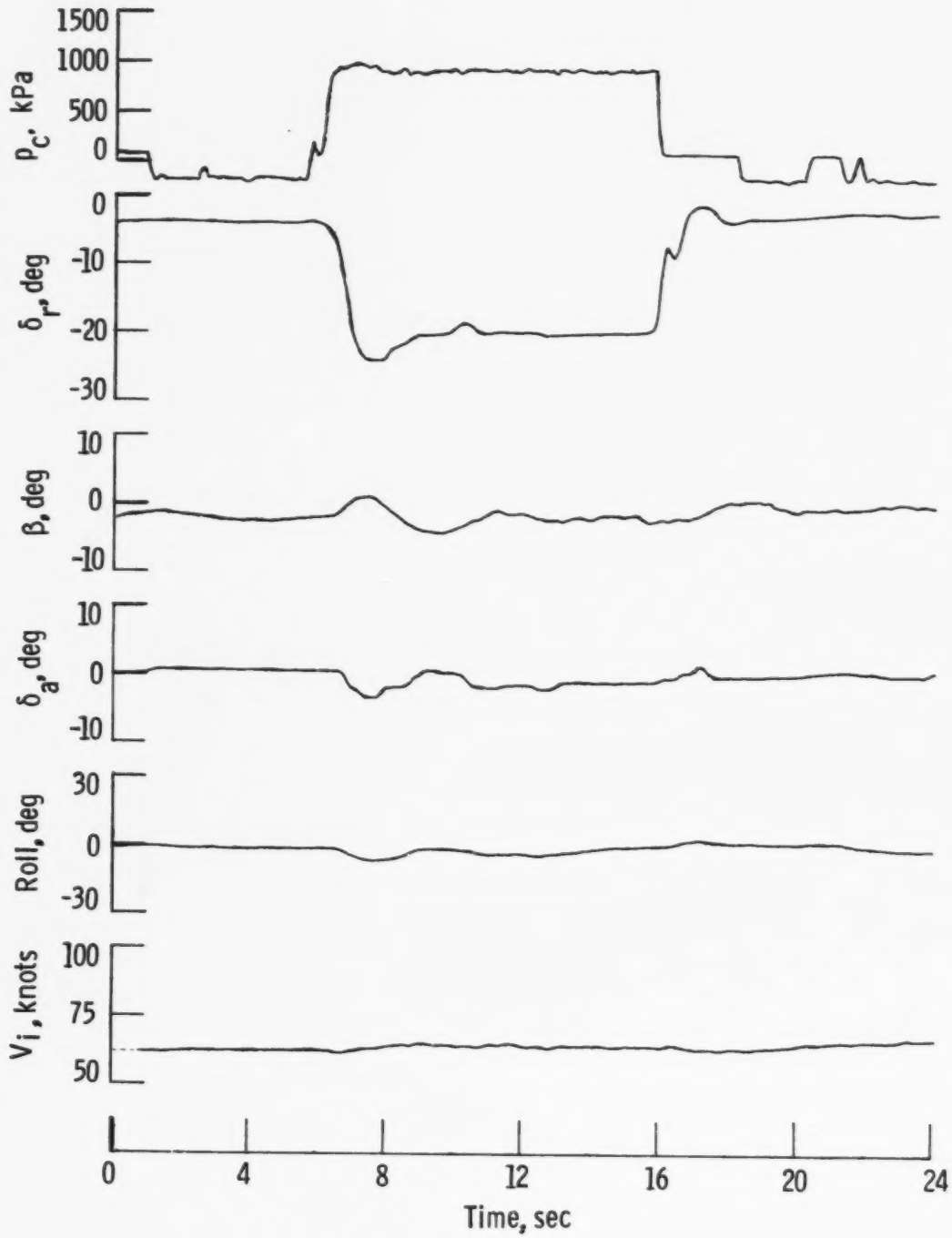

Figure 12.- Time history of yaw rocket-firing maneuver.

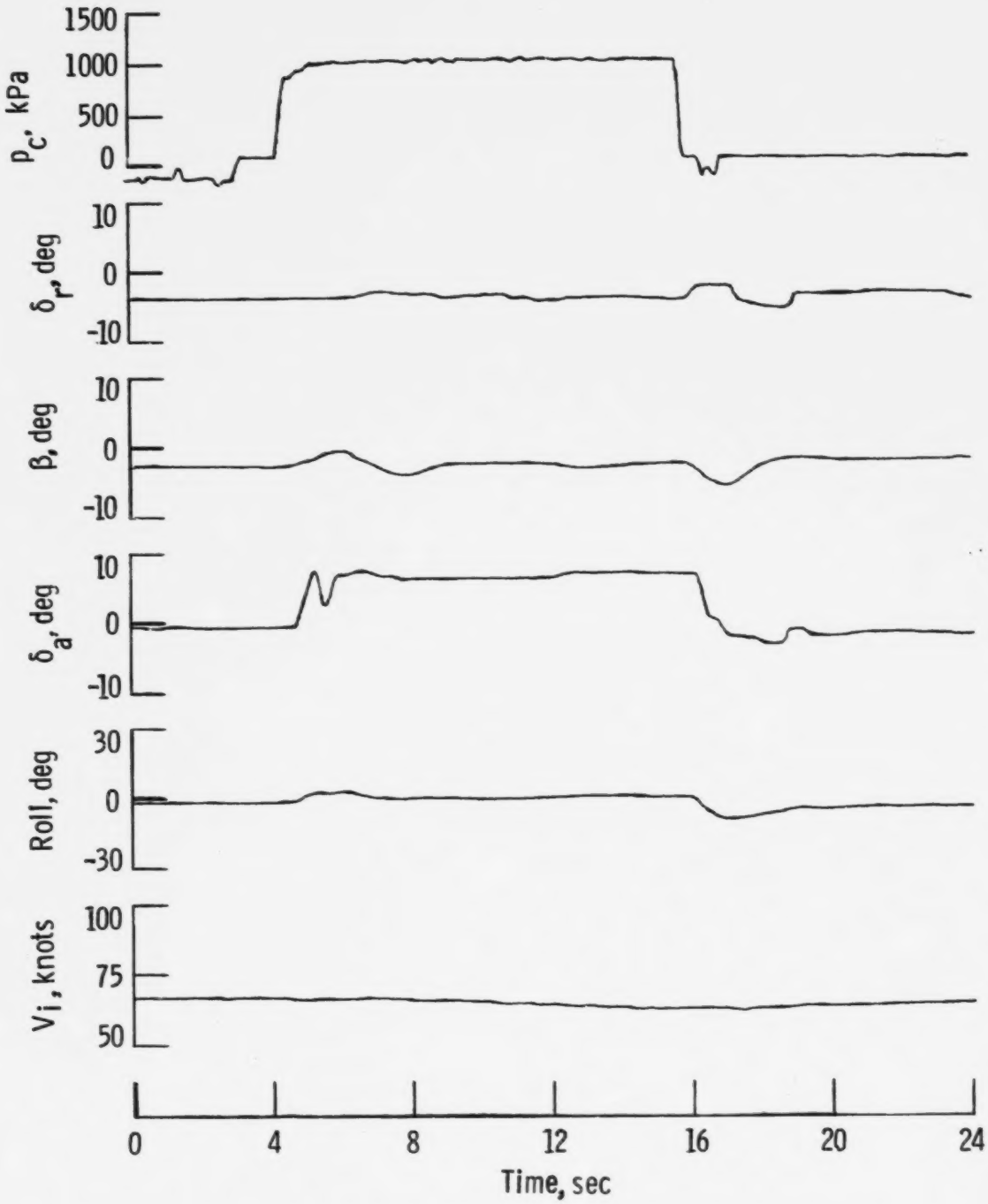

Figure 13.- Time history of the roll rocket-firing maneuver.

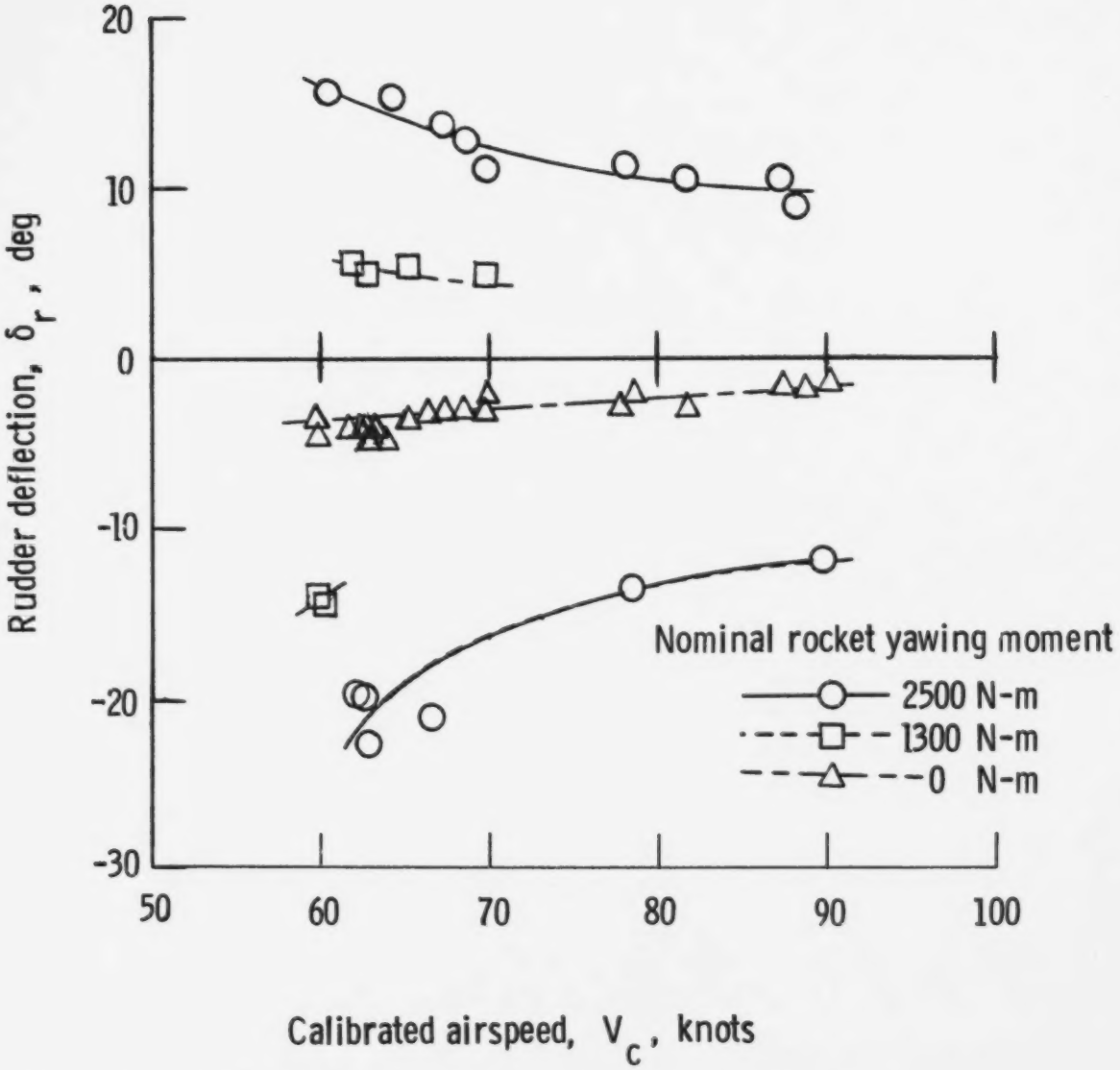

Figure 14.- Rudder deflection required to balance rocket yawing moment with power for level flight.

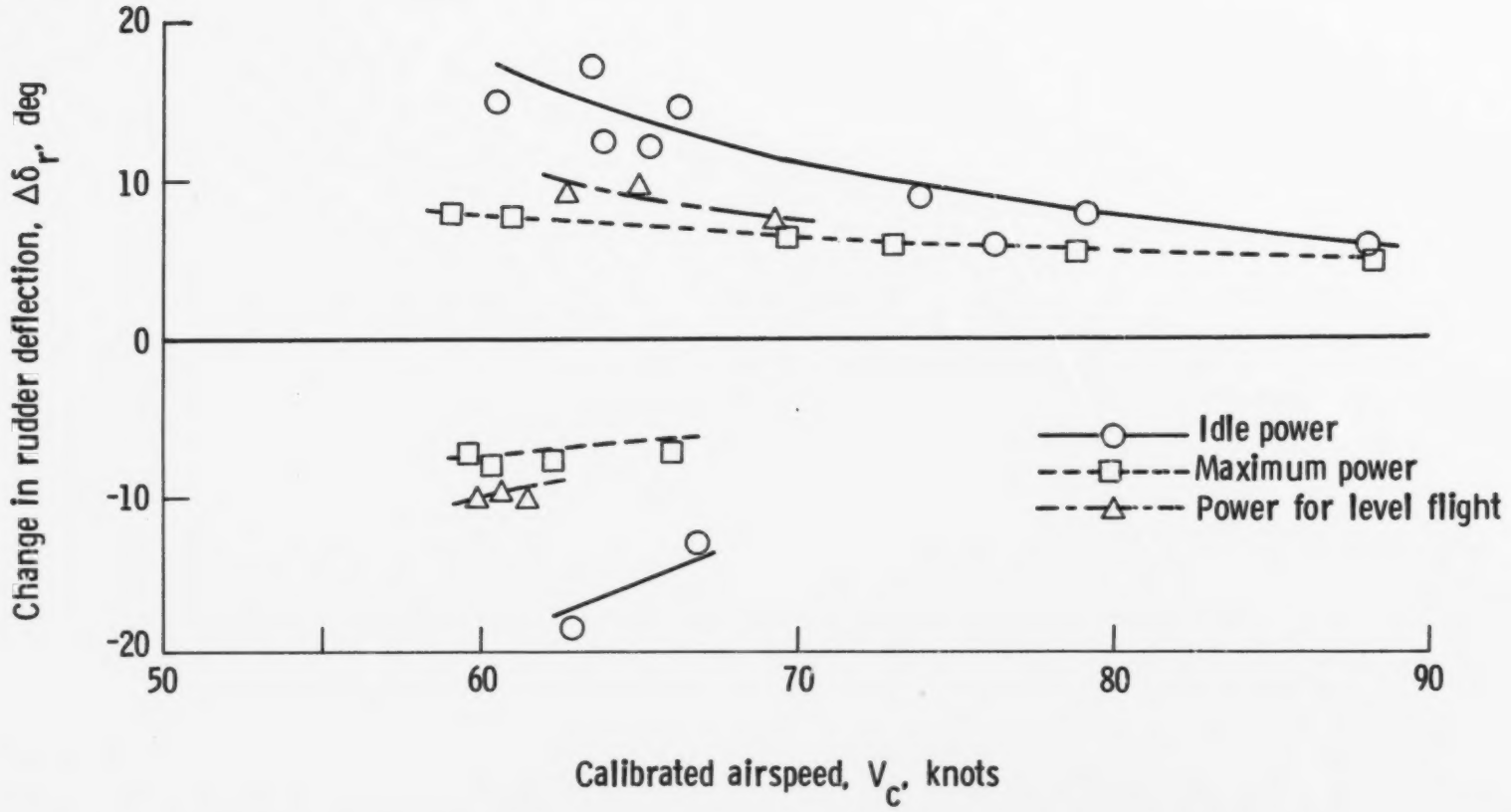

Figure 15.- Change in rudder deflection required to balance minimum rocket yawing moment for all power conditions.

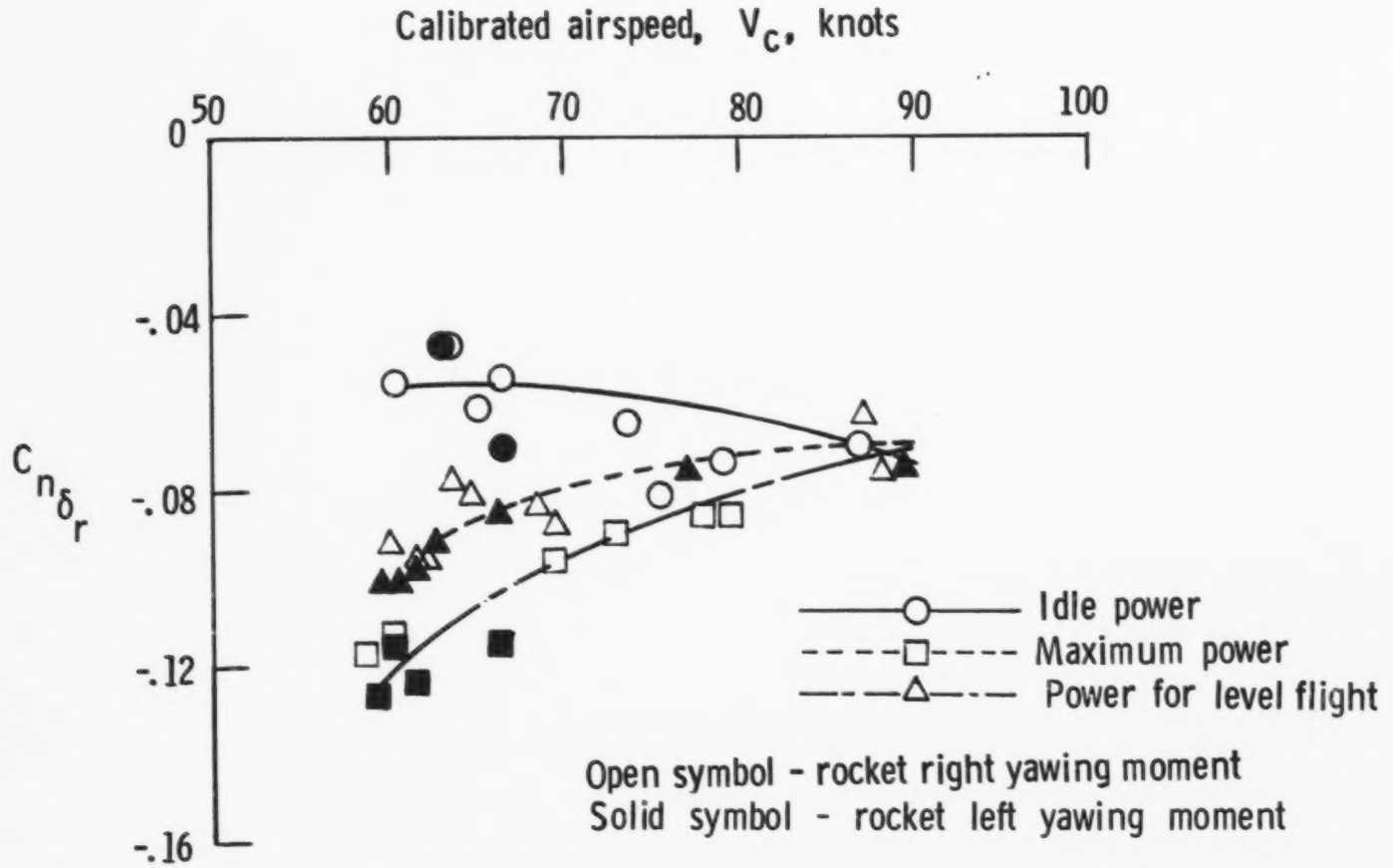

Figure 16.- Rudder effectiveness for all power conditions.

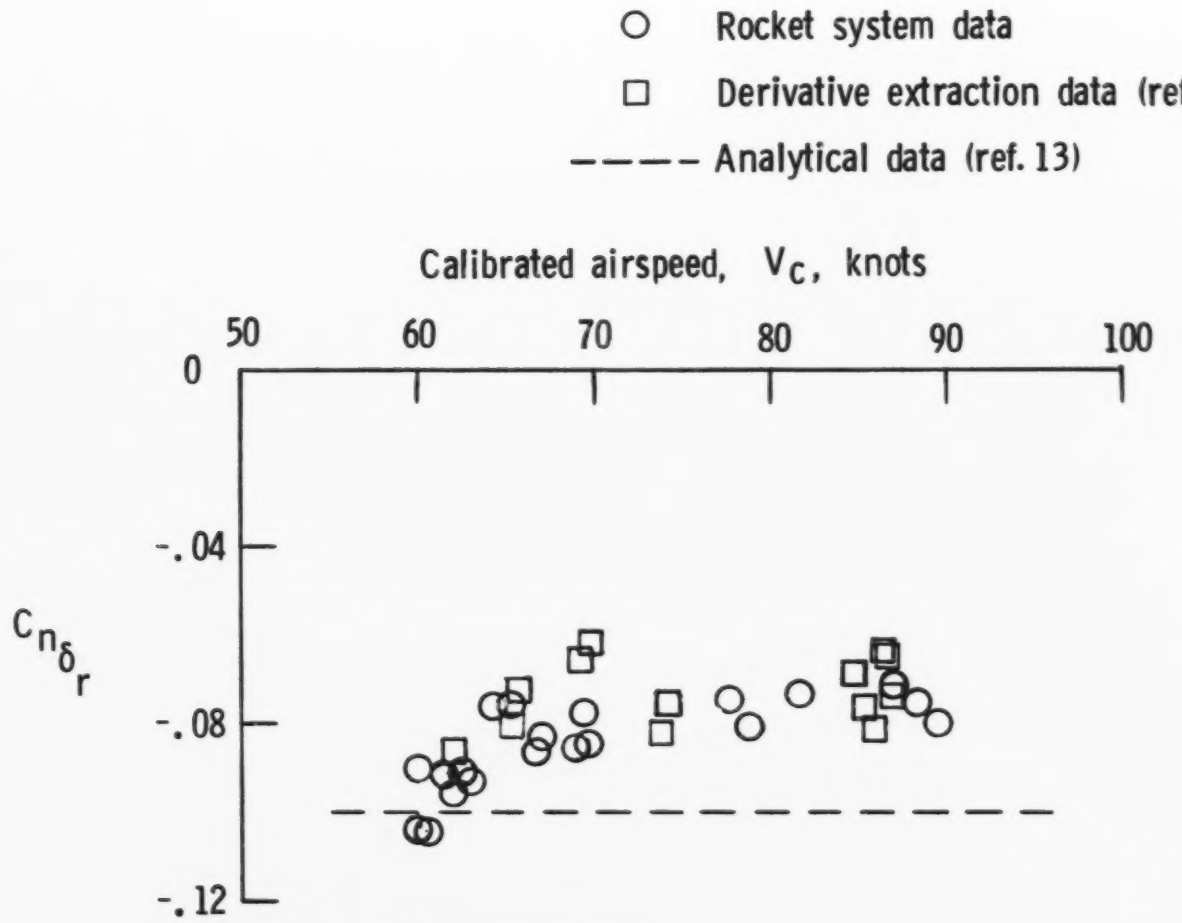

Figure 17.- Rudder effectiveness with power for level flight.

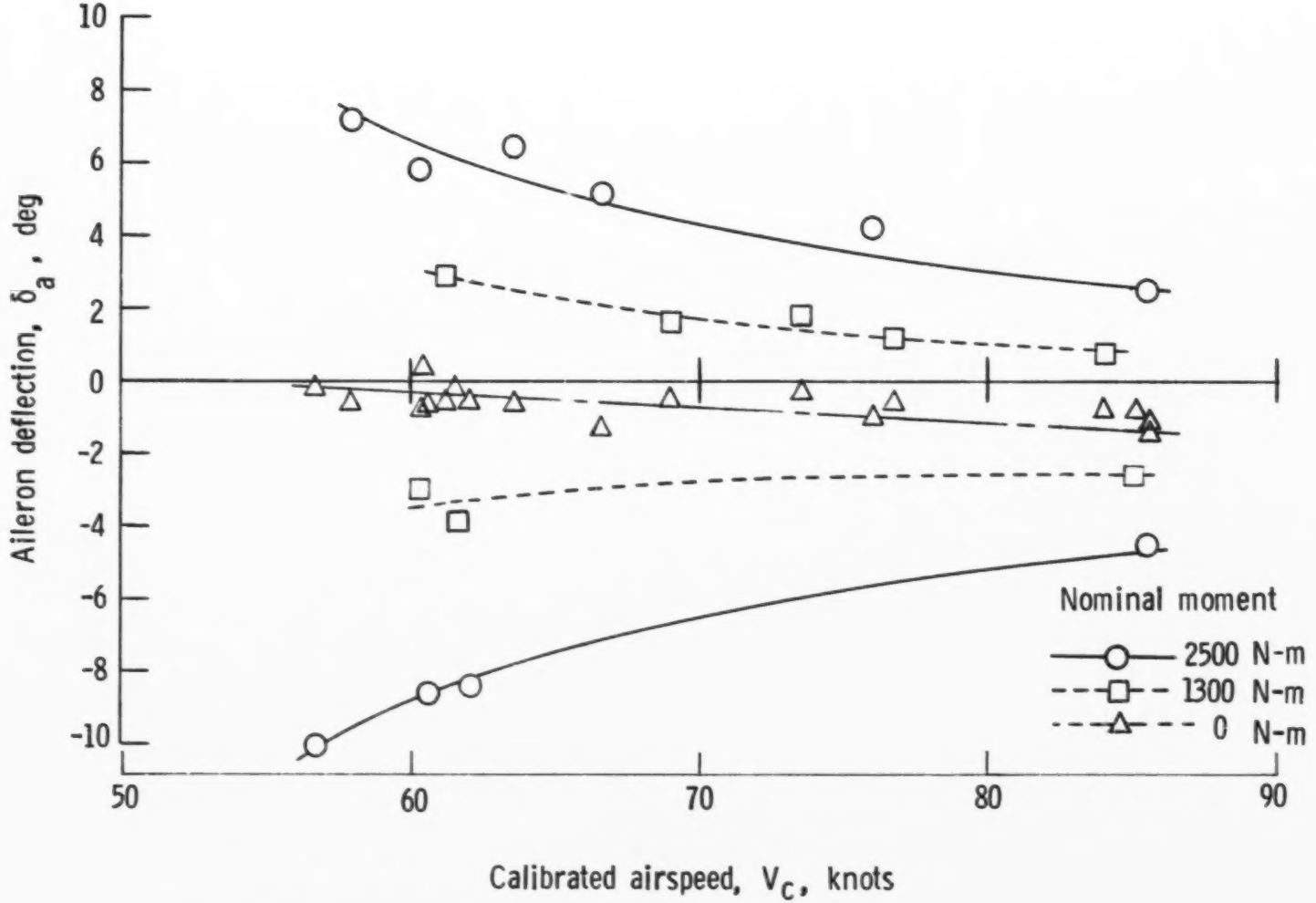

Figure 18.- Aileron deflection required to balance rolling moment.

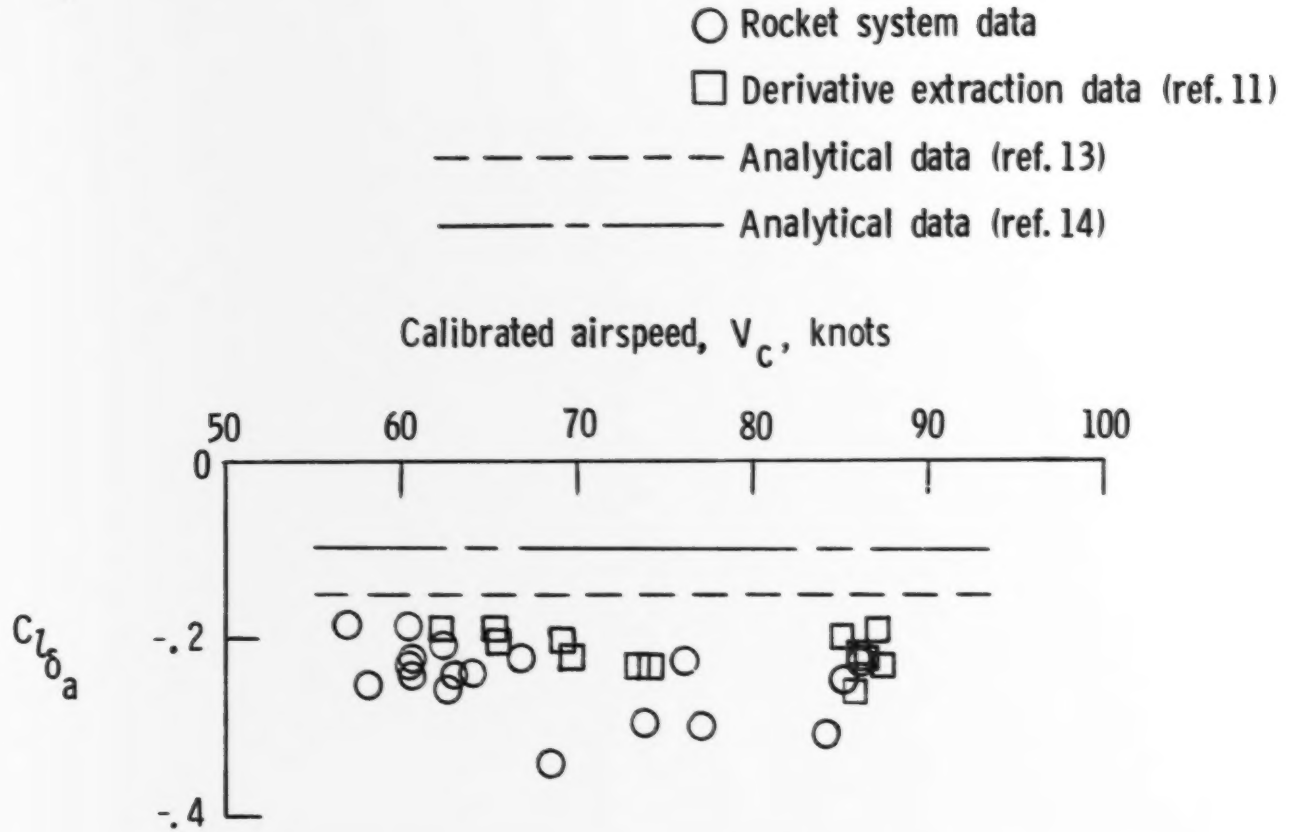

Figure 19.- Aileron effectiveness compared with theory and with derivative extraction data. Power for level flight.

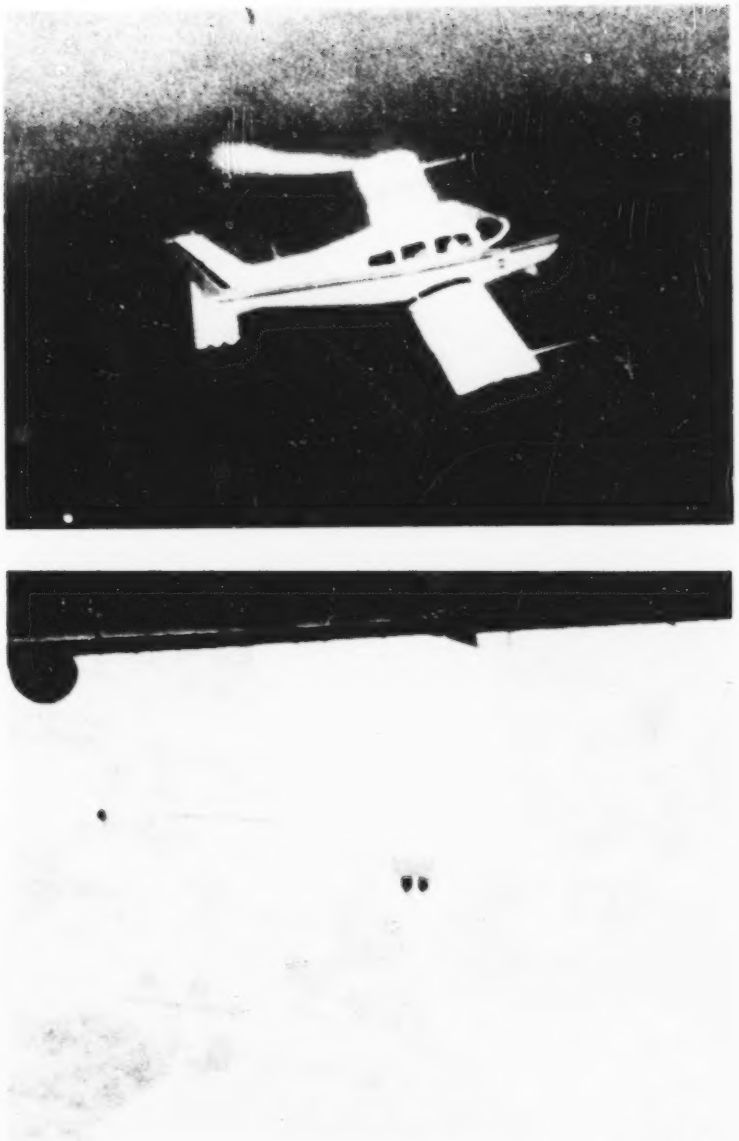

L-80-123

Figure 20.- Rocket motor exhaust plume during motor warmup.

1. Report No.	2. Government Accession No.	3. Recipient's Catalog No.
NASA TP-1647		

4. Title and Subtitle	5. Report Date
DESCRIPTION OF AN EXPERIMENTAL (HYDROGEN PEROXIDE) ROCKET SYSTEM AND ITS USE IN MEASURING AILERON AND RUDDER EFFECTIVENESS OF A LIGHT AIRPLANE	May 1980
	6. Performing Organization Code

7. Author(s)	8. Performing Organization Report No.
Thomas C. O'Bryan, Maxwell W. Goode, Frederick D. Gregory, and Marna H. Mayo	L-12494
	10. Work Unit No. 505-41-13-03
9. Performing Organization Name and Address NASA Langley Research Center Hampton, VA 23665	11. Contract or Grant No.
	13. Type of Report and Period Covered Technical Paper
12. Sponsoring Agency Name and Address National Aeronautics and Space Administration Washington, DC 20546	14. Sponsoring Agency Code

15. Supplementary Notes

16. Abstract

A hydrogen-peroxide-fueled rocket system which is to be used as a research tool in flight studies of stall and spin maneuvers was installed on a light, four-place general aviation airplane. The pilot-controlled rocket system produces moments about either the roll or the yaw body axis to augment or oppose the aerodynamic forces and inertial moments acting on the airplane during various flight maneuvers, including the spin. These controlled moments of a known magnitude can be used in various ways to help analyze and interpret the importance of the various factors which influence airplane maneuvers. This paper describes the rocket system and its installation in the airplane and presents the results of flight tests used to measure rudder and aileron effectiveness at airspeeds above the stall. These tests also serve to demonstrate the operational readiness of the rocket system for future research operations.

17. Key Words (Suggested by Author(s))	18. Distribution Statement
Spinning Rockets Stability derivatives	Unclassified - Unlimited Subject Category 08

19. Security Classif. (of this report)	20. Security Classif. (of this page)	21. No. of Pages	22. Price*
Unclassified	Unclassified	39	$4.50

* For sale by the National Technical Information Service, Springfield, Virginia 22161

NASA-Langley, 1980